Thermal dissipation field and its statistics in turbulent Rayleigh-Bénard convection

Penger Tong

Department of Physics
Hong Kong University of Science and Technology

OUTLINE:

1. Dissipations in Rayleigh-Bénard convection
2. Measurement of the local thermal dissipation rate
3. Experimental results
4. Summary

Work done in collaboration with Xiao-zhou He and Emily Ching and was supported by Hong Kong Research Grants Council

KITP Program on the Nature of Turbulence, April 6, 2011

1. Dissipations in Rayleigh-Bénard Convection

For turbulent Rayleigh-Bénard convection, we have

• three local variables, $\mathbf{v}(\mathbf{r},t)$, $T(\mathbf{r},t)$ and $p(\mathbf{r},t)$, and three equations:

$$\frac{\partial \mathbf{v}}{\partial t} + \mathbf{v}\cdot\nabla\mathbf{v} = -\frac{1}{\rho}\nabla p + \nu\nabla^2\mathbf{v} - \mathbf{g}\alpha\delta T$$

$$\frac{\partial T}{\partial t} + \mathbf{v}\cdot\nabla T = \kappa\nabla^2 T$$

$$\nabla\cdot\mathbf{v} = 0$$

Flow visualization of turbulent thermal convection in water

• two corresponding dissipation rates, ε_u and ε_T.

There are two exact relations:

$$\varepsilon_T = \kappa \langle [\partial_i T(\mathbf{r},t)]^2 \rangle_{V,t} = \kappa (\Delta T / H)^2 Nu(Ra, \mathrm{Pr})$$

$$\varepsilon_u = \nu \langle [\partial_i \mathbf{v}_j(\mathbf{r},t)]^2 \rangle_{V,t} = (\nu^3 / H^4)(Nu - 1) Ra\, \mathrm{Pr}^{-2}$$

- Understanding heat transport, Nu(Ra,Pr), in turbulent convection through spatial decomposition of the dissipation fields ε_u and ε_T

Phenomenology of Grossmann & Lohse (JFM, 2000; PoF, 2004):

boundary *versus* bulk

$$\boxed{\varepsilon_u = \varepsilon_{u,BL} + \varepsilon_{u,bulk}} \qquad \boxed{\varepsilon_T = \varepsilon_{T,BL} + \varepsilon_{T,bulk}}$$

$$\varepsilon_{u,BL} \sim \nu (u/\lambda_u)^2 (\lambda_u / H) \qquad \varepsilon_{T,BL} \sim \kappa (\Delta T / \lambda_T)^2 (\lambda_T / H)$$

$$\varepsilon_{u,bulk} \sim u^3 / H \qquad \varepsilon_{T,bulk} \sim (u\varphi) \Delta T^2 / H$$

- Understanding small-scale properties of turbulent convection through the statistics of dissipation fluctuations ε_u and ε_T

Kolmogorov refined similarity hypothesis (JFM, 1962)

$$S_u^{(p)}(r) = \left\langle \left([\mathbf{u}(x+r,t) - \mathbf{u}(x,t)] \bullet \frac{\mathbf{r}}{r} \right)^p \right\rangle_t \sim r^{\varsigma_p} \sim \langle \varepsilon_u(r)^{p/3} \rangle r^{p/3}$$

$$S_T^{(p)}(r) = \left\langle [T(x+r,t) - T(x,t)]^p \right\rangle_t \sim r^{\xi_p} \sim \langle \varepsilon_u(r)^{-p/6} \rangle \langle \varepsilon_T(r)^{p/2} \rangle r^{p/3}$$

Scale-dependent fluctuations of $\varepsilon_u(\mathbf{r},t)$ and $\varepsilon_T(\mathbf{r},t)$ will give rise to anomalous scaling for the velocity and temperature structure functions.

X.-Z. He, P. Tong & K-Q. Xia, *Phys. Rev. Lett.* **98**, 144501 (2007).

X.-Z. He & P. Tong, *Phys. Rev. E* **79**, 026306 (2009).

X.-Z. He, P. Tong & E. Ching, *J. Turbulence*, **11**, No. 35, 1 (2010).

X.-Z. He, E. Ching, & P. Tong, *Phys. Fluids* **23**, 025106 (2011).

2. Measurement of the local thermal dissipation rate

Instantaneous local viscous dissipation rate:

$$\varepsilon_u(\mathbf{r},t) = \nu \sum_{i,j} \frac{\partial u_i}{\partial x_j}\frac{\partial u_i}{\partial x_j}$$

Instantaneous local thermal dissipation rate:

$$\varepsilon_T(\mathbf{r},t) = \kappa[(\frac{\partial T}{\partial x})^2 + (\frac{\partial T}{\partial y})^2 + (\frac{\partial T}{\partial z})^2]$$

Time-averaged local thermal dissipation rate:

$$\langle\varepsilon_T(\mathbf{r},t)\rangle_t \simeq (\varepsilon_T)_m(\mathbf{r}) + (\varepsilon_T)_f(\mathbf{r}) = \kappa\sum_i \langle(\frac{\partial \overline{T}}{\partial x_i})^2\rangle_t + \kappa\sum_i \langle(\frac{\partial \tilde{T}}{\partial x_i})^2\rangle_t$$

Total convective heat flux across the cell:

$$\mathrm{Nu} = \frac{1}{A}\iint \mathrm{J_z}(x,y)dxdy = \frac{1}{\kappa(\Delta T/H)^2}\frac{1}{V}\iiint\langle\varepsilon_T(\mathbf{r},t)\rangle_t d\mathbf{r}$$

Local temperature gradient probe:

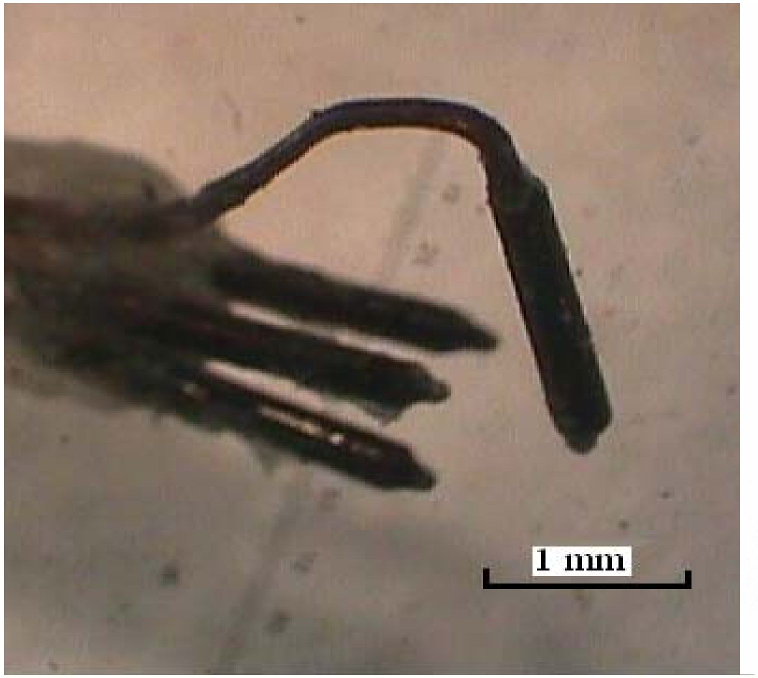

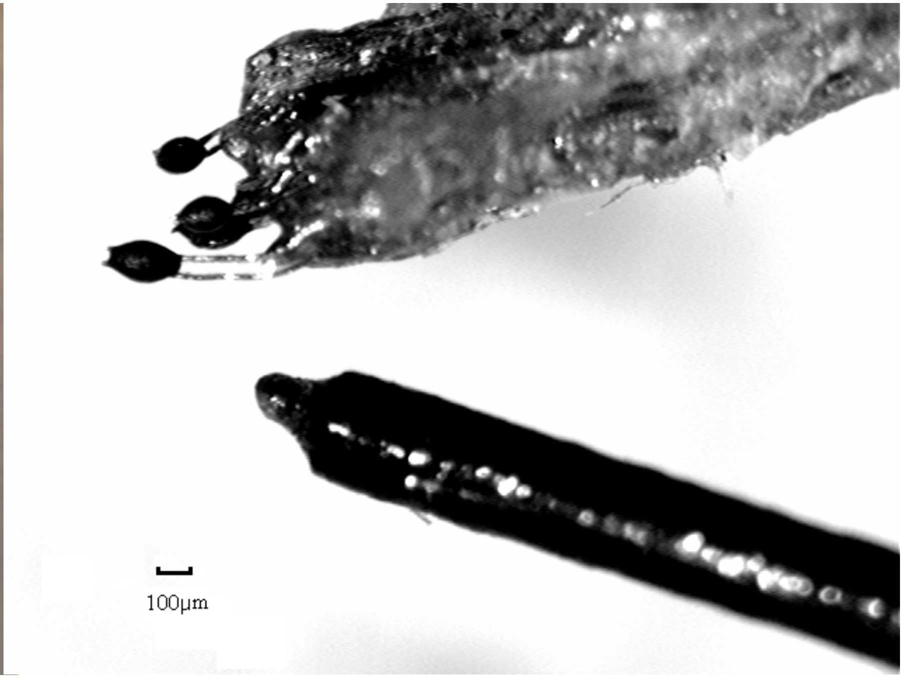

First probe: d = 0.17 mm

$\delta x_i = 0.8$ mm, $\delta T_{min} \approx 5$ mK

Second probe: d = 0.11 mm

$\delta x_i = 0.25$ mm, $\delta T_{min} \approx 5$ mK

$\delta \approx 0.8$ mm at $Ra = 3.6\times 10^9$

Rayleigh-Bénard convection cell

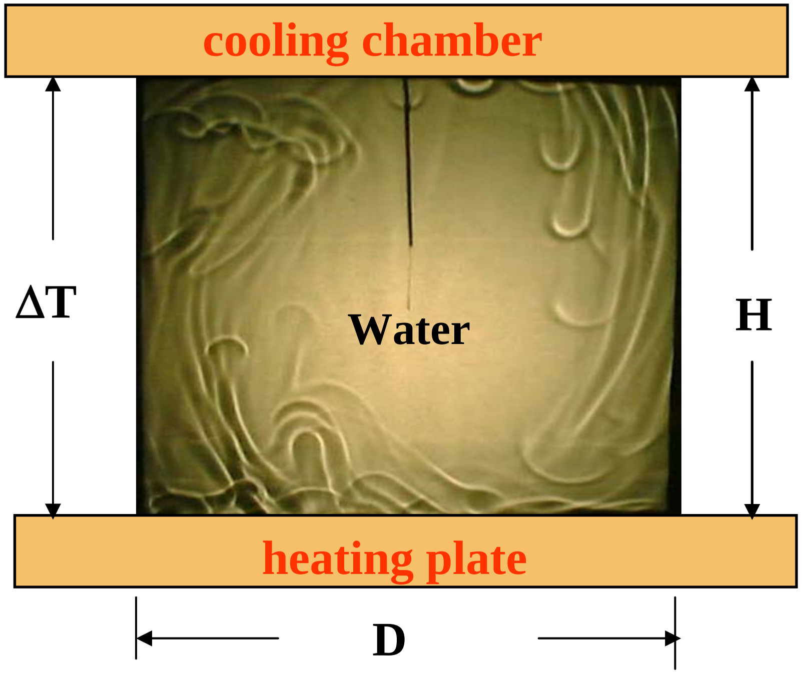

$$Ra = \frac{\alpha g H^3 \Delta T}{\nu \kappa}$$

$$(10^8 \leq Ra \leq 10^{10})$$

$$\Delta T \simeq 1 \text{ to } 40^\circ C$$

$$\Pr = \frac{\nu}{\kappa} \approx 5.4$$

$$\Gamma = \frac{D}{H} = 1 \text{ and } 0.5$$

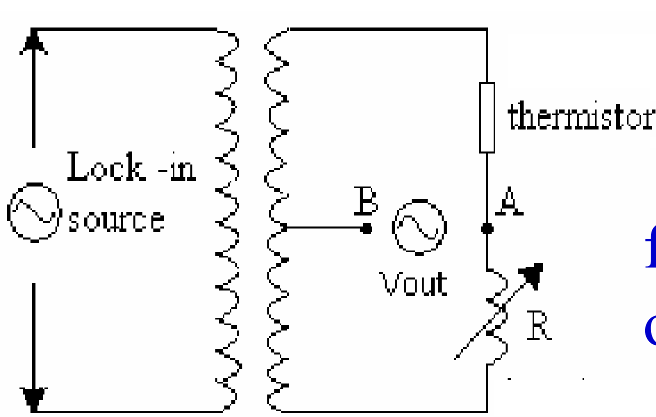

four ac bridges with lock-in amplifiers operated at f ≈ 1 kHz and Δf = 100 Hz

3. Experimental results

A. Spatial distribution of the thermal dissipation field

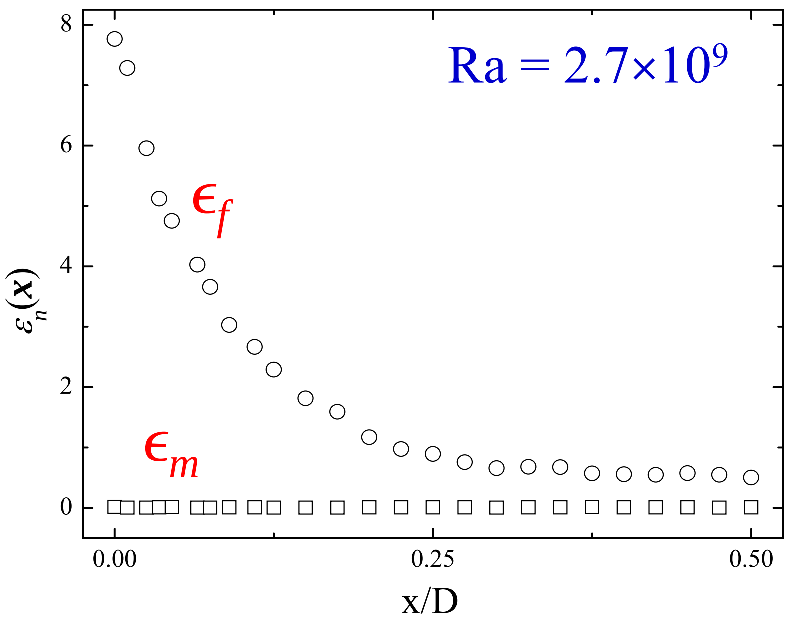

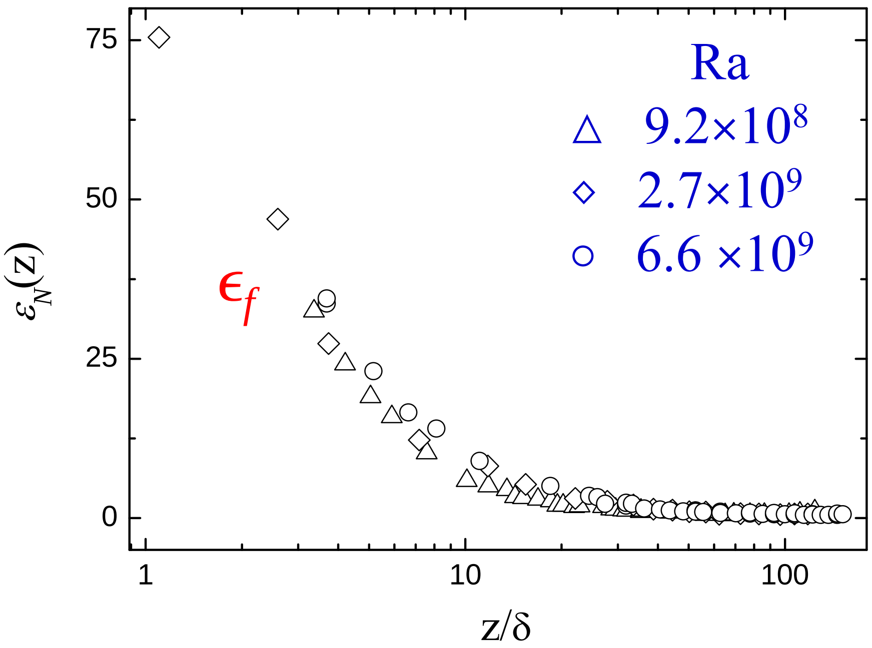

$$\boxed{\varepsilon_N(\mathbf{r}) = \varepsilon_m(\mathbf{r}) + \varepsilon_f(\mathbf{r})}$$

(i) In the bulk region, ϵ_f is dominant and ϵ_m is negligibly small.

(ii) ϵ_f increases rapidly in the $1 \le z/\delta \le 10$ region and is ~140 times larger than that at the cell center.

$\mathrm{Ra} = 3.9\times10^9$

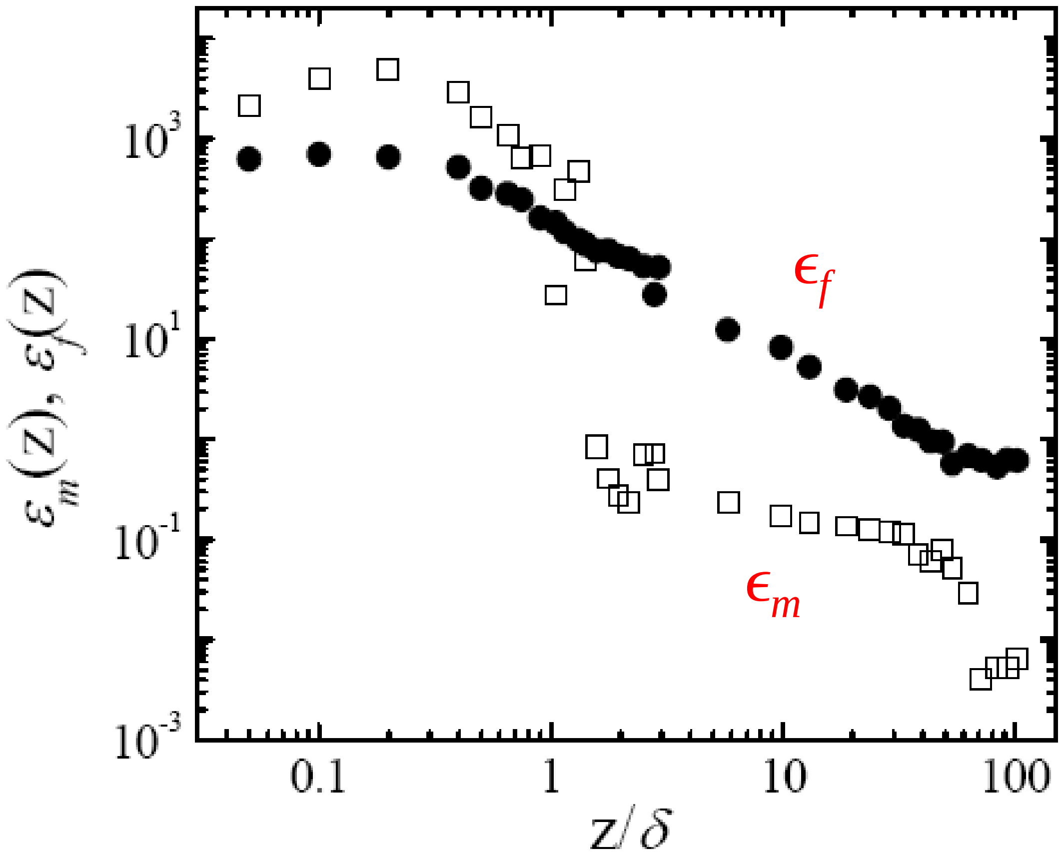

(iii) In the thermal boundary layer, ϵ_m becomes dominant and ϵ_f is smaller.

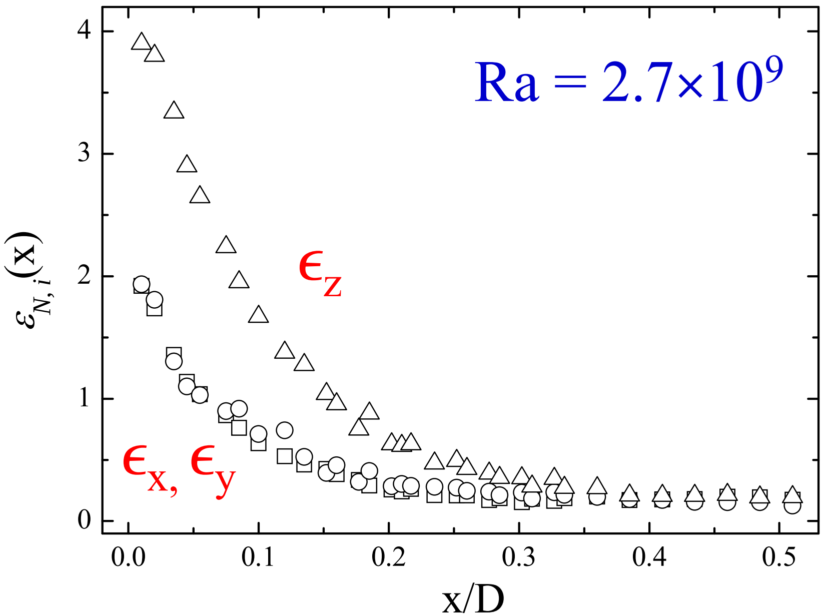

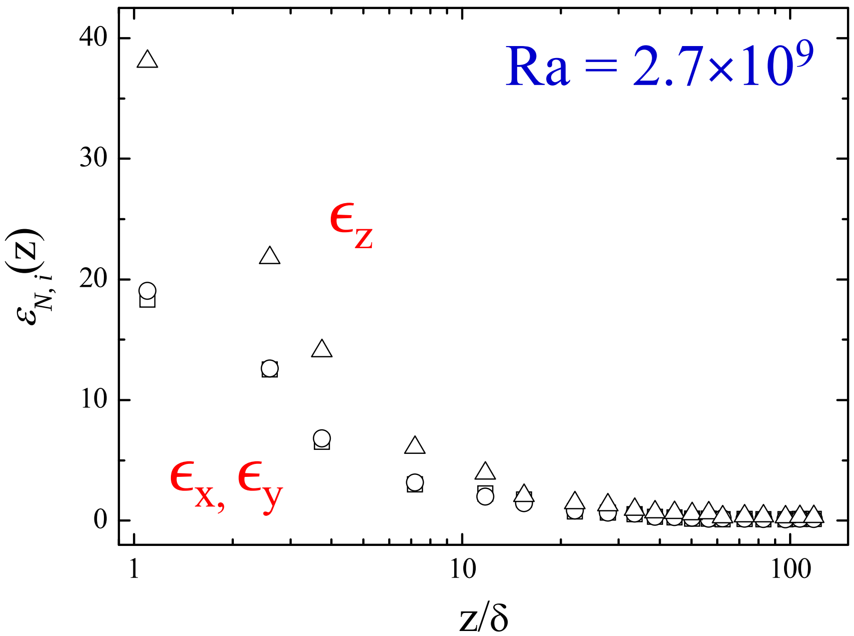

(iv) ϵ_f has three terms, $\epsilon_f = \epsilon_x + \epsilon_y + \epsilon_z$, and the dominant term is ϵ_z, which is twice larger than ϵ_x and ϵ_y.

B. Ra-dependence of the local thermal dissipation rate

At the cell center

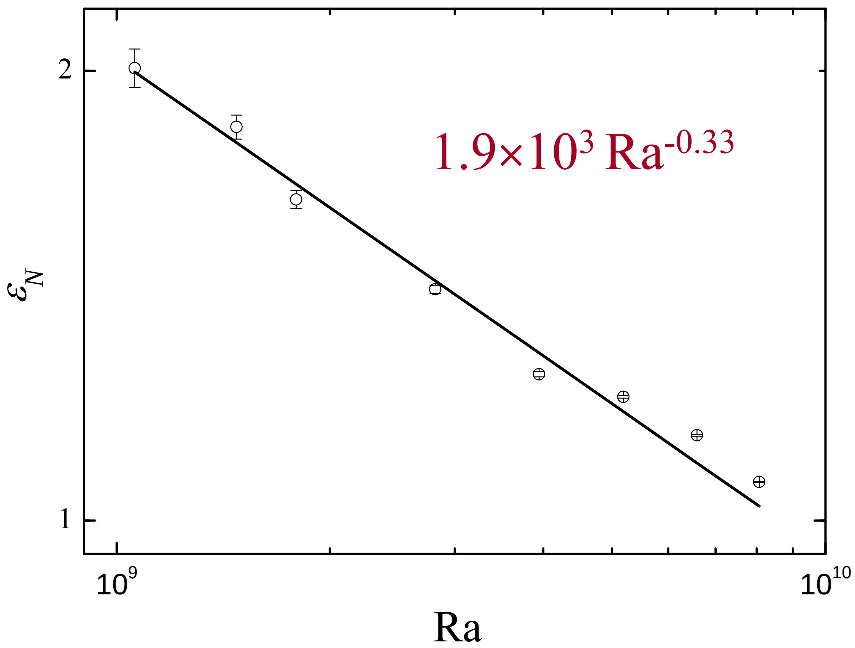

Near the sidewall

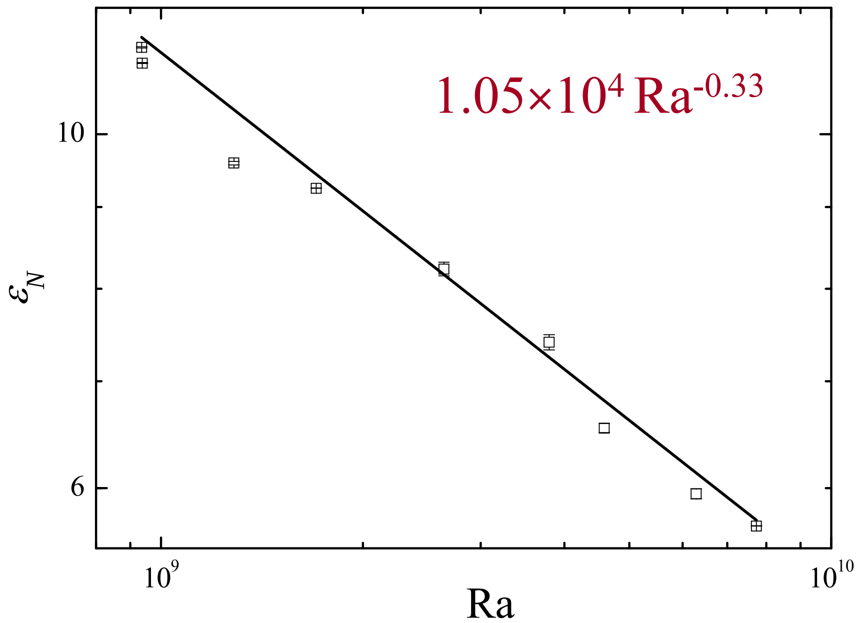

(v) $\epsilon_f \sim Ra^{-\alpha}$ with $\alpha = 0.33 \pm 0.03$ both at the cell center and near the sidewall.

Inside the thermal boundary layer (almost touching the lower surface)

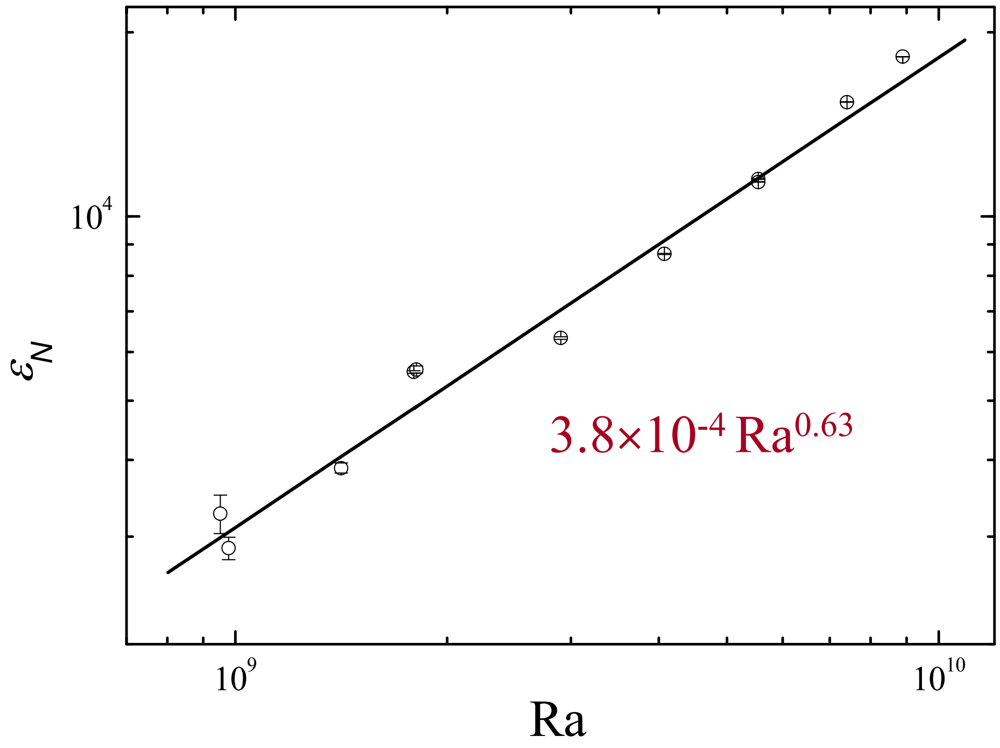

(vi) $\epsilon_m \sim Ra^{+\beta}$ with $\beta = 0.63 \pm 0.05$ inside the thermal boundary layer.

C. Scale-dependent statistics of dissipation fluctuations ϵ_f (r,t)

Near the sidewall at Ra = 3.6×10^9

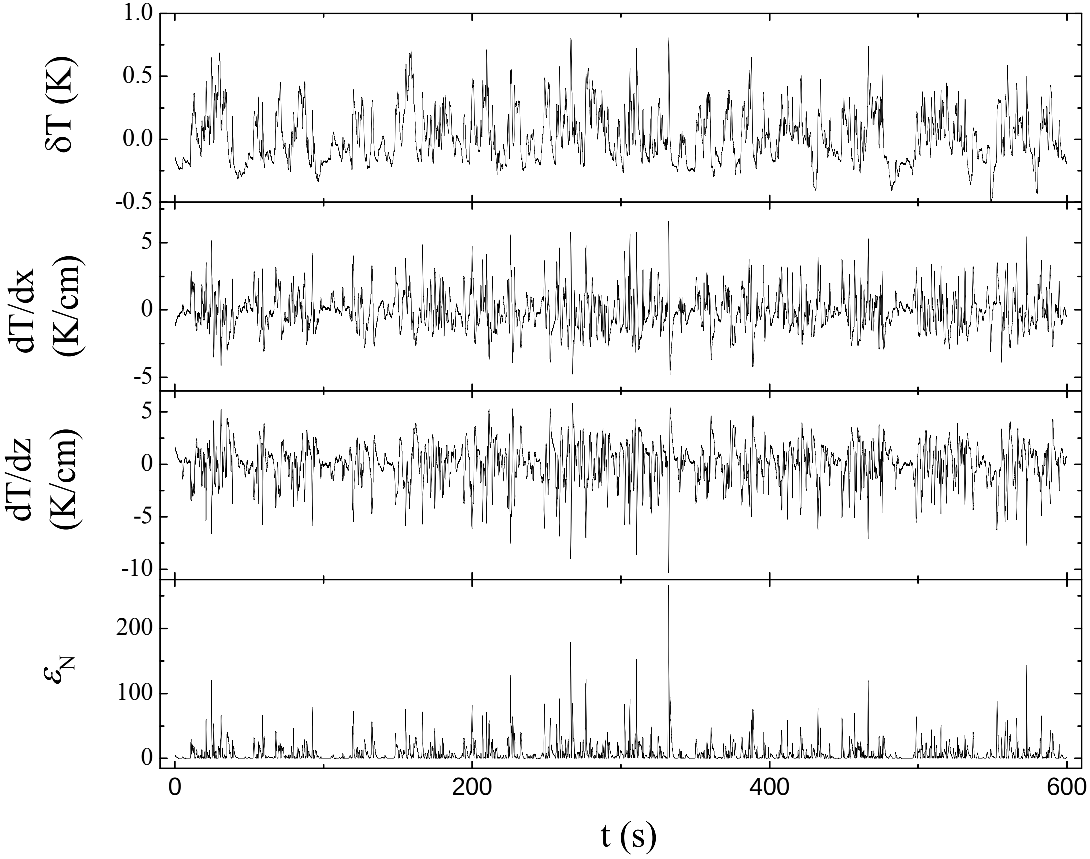

asymmetric

symmetric

slightly asymmetric

asymmetric

Histogram of the three temperature gradient components

At the cell center

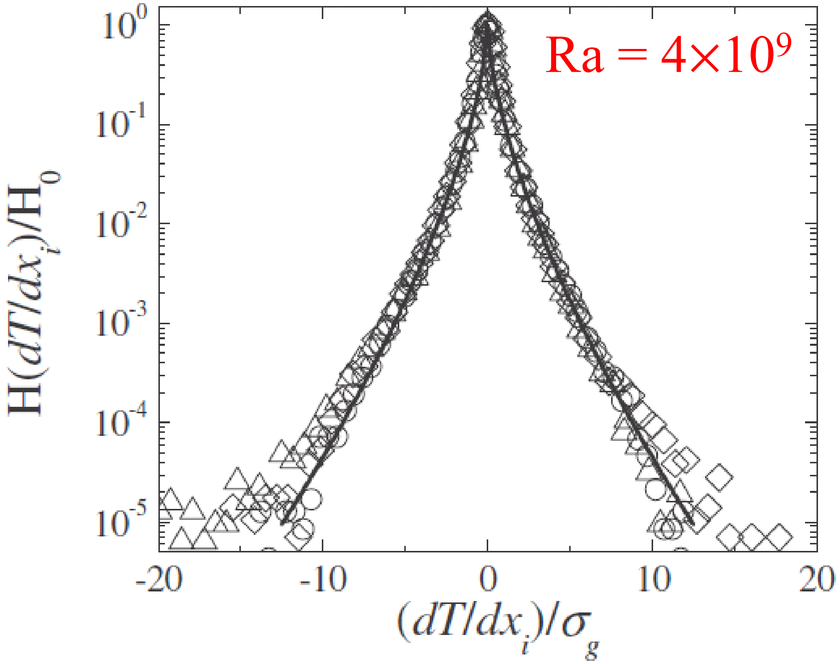

Approximately isotropic

Near the sidewall

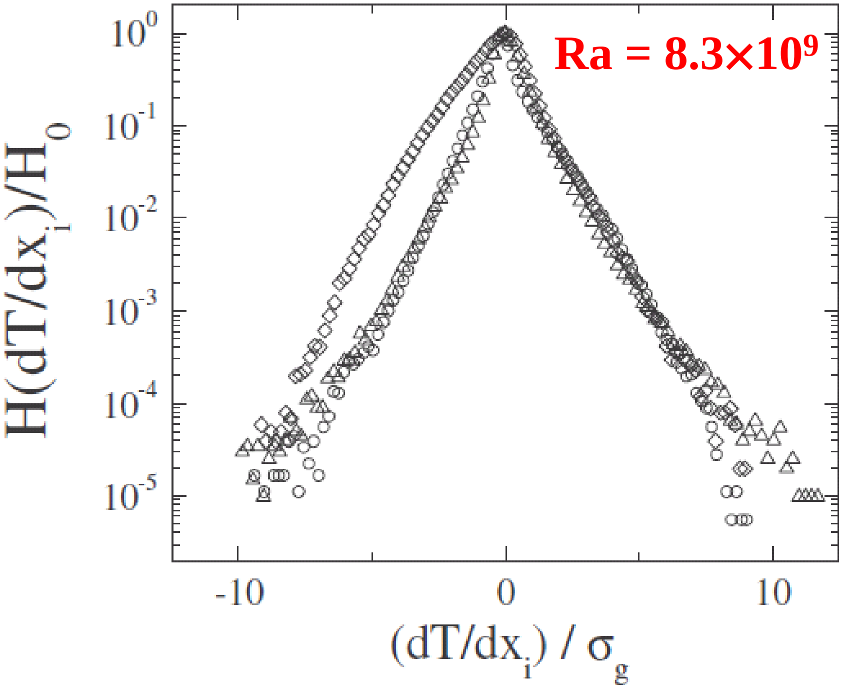

Anisotropic fluctuations

Challenges in identifying anomalous scaling in turbulent convection

- Convective flow in a closed cell is neither homogeneous nor isotropic

  - three representative locations in the cell:

  at the center, near the sidewall and near the lower conducting plate

  - decomposition of the local dissipation rate into contributions

  from three different temperature gradient components.

- Bolgiano length and separation of passive and active scalars within a limited range of length scales

$$L_B \simeq Nu^{1/2}(\mathrm{Pr}\,Ra)^{-1/4}L \simeq 6.3\ mm; \qquad L_B(z) \simeq \varepsilon_u^{5/4}(z)\varepsilon_T^{-3/4}(z)(\alpha g)^{-3/2}$$

- Connection of time-domain results to the theory in spatial domain

  Taylor's frozen-flow hypothesis does not hold in turbulent convection

Lohse & Xia, Annu. Rev. Fluid Mech. (2010)

Scale-dependent statistics of the locally averaged $\epsilon_\tau(\mathbf{r},t)$

$$\varepsilon_T(\mathbf{r},t) = \kappa[|\nabla T_m(r)|^2 + 2\nabla T_m(\mathbf{r})\bullet\nabla T_f(\mathbf{r},t) + |\nabla T_f(\mathbf{r},t)|^2]$$

$$\varepsilon_\tau^i(\mathbf{r},t) = \frac{1}{\tau}\int_t^{t+\tau}\kappa[\partial_i T_f(\mathbf{r},t')]^2\,dt'$$

$$\langle(\varepsilon_\tau^i)^p\rangle \equiv \langle[\varepsilon_\tau^i(\mathbf{r},t)]^p\rangle_t \sim \tau^{\mu^i(p)}$$

Assuming $\langle(\varepsilon_\tau^i)^p\rangle$ has a hierarchical structure of the She–Leveque form, one finds

[Ching & Kwok, PRE **62,** 7587(R) (2000)]

$$\mu^i(p) = c(1-\beta^p) - \lambda p$$

where $c = 3 - D_\epsilon$ is co-dimension of the most dissipative structures, $\lambda = 1 - b$ (for velocity scaling) and

$$0 = c(1-\beta) - \lambda$$

For passive scalars with sheet-like dissipative structures:

$$\lambda = \frac{2}{3}, \quad c = 1 \quad \text{and } \beta = \frac{1}{3}$$

(central region)

For passive scalars with filament-like dissipative structures:

$$\lambda = \frac{2}{3}, \quad c = 2 \quad \text{and } \beta = \frac{2}{3}$$

(vertical exponent in the sidewall region)

For active scalars with sheet-like dissipative structures:

$$\lambda = \frac{2}{5}, \quad c = 1 \quad \text{and } \beta = \frac{3}{5}$$

(inside the thermal boundary layer)

Scaling of $\langle(\varepsilon_\tau^z)^p\rangle$ at the cell center:

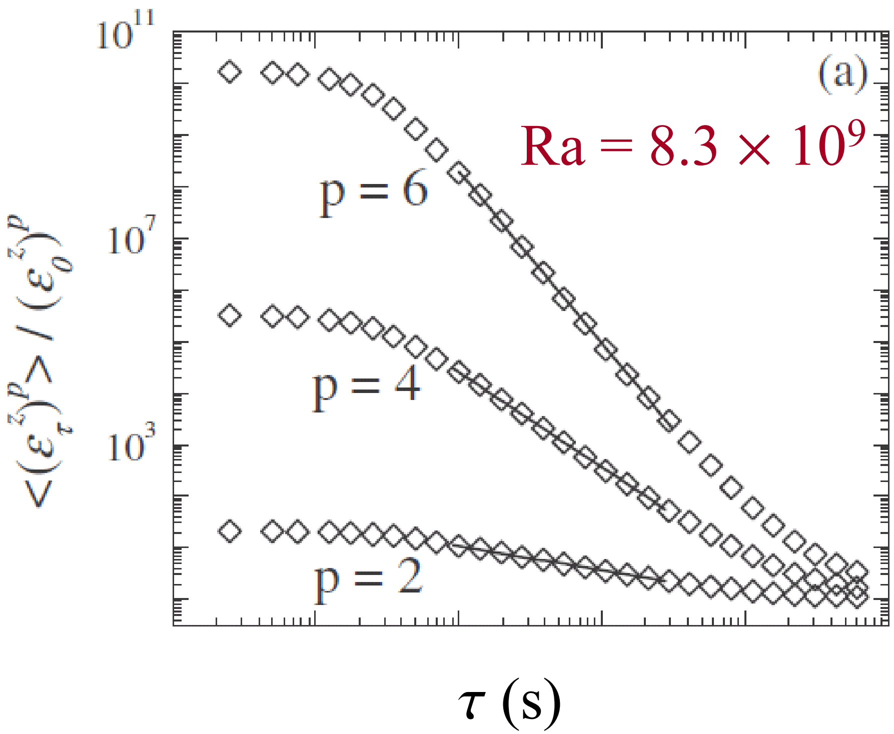

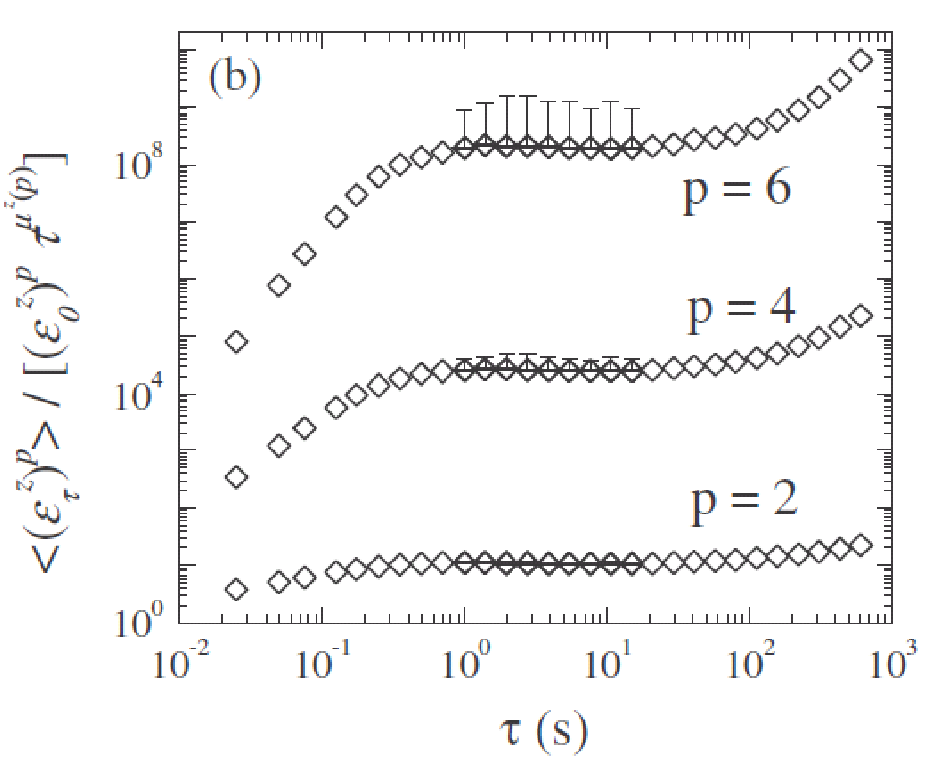

LSC turnover time $\tau_0 \approx 35$ s; local Bolgiano time $\tau_B \approx \tau_0\, L_B(z)/L \approx 31$ s.

Dissipation time $\tau_d = \tau_0\, (10\eta)/L \approx 0.8$ s.

Convergence and accuracy of the measured $\langle (\varepsilon_\tau^z)^p \rangle$

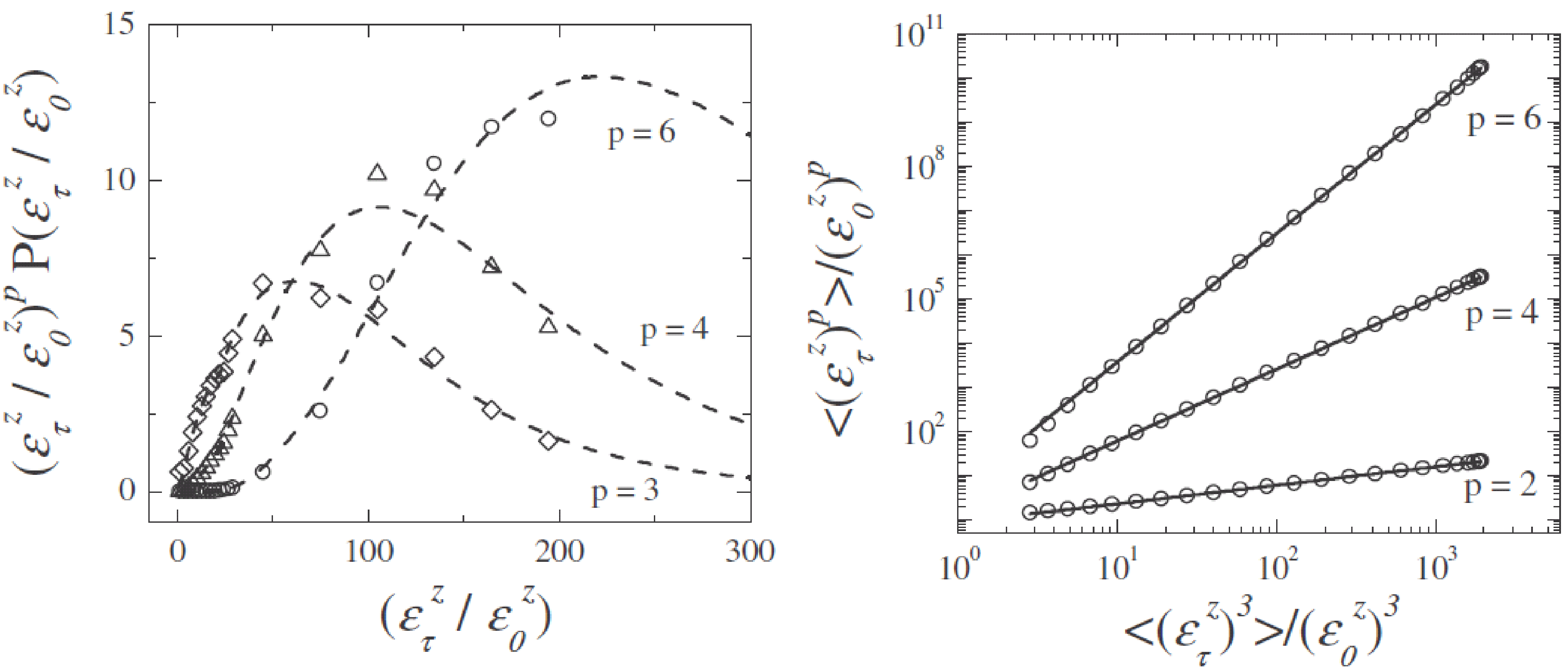

$$\frac{\langle (\varepsilon_\tau^z)^p \rangle}{(\varepsilon_0^z)^p} \simeq \frac{1}{\varepsilon_0^z} \int_0^\infty (\varepsilon_\tau^z / \varepsilon_0^z)^p P(\varepsilon_\tau^z / \varepsilon_0^z) d\varepsilon_\tau^z$$

Extended self-similarity (ESS) plots

Scaling exponent $\mu^z(p)$ at the cell center:

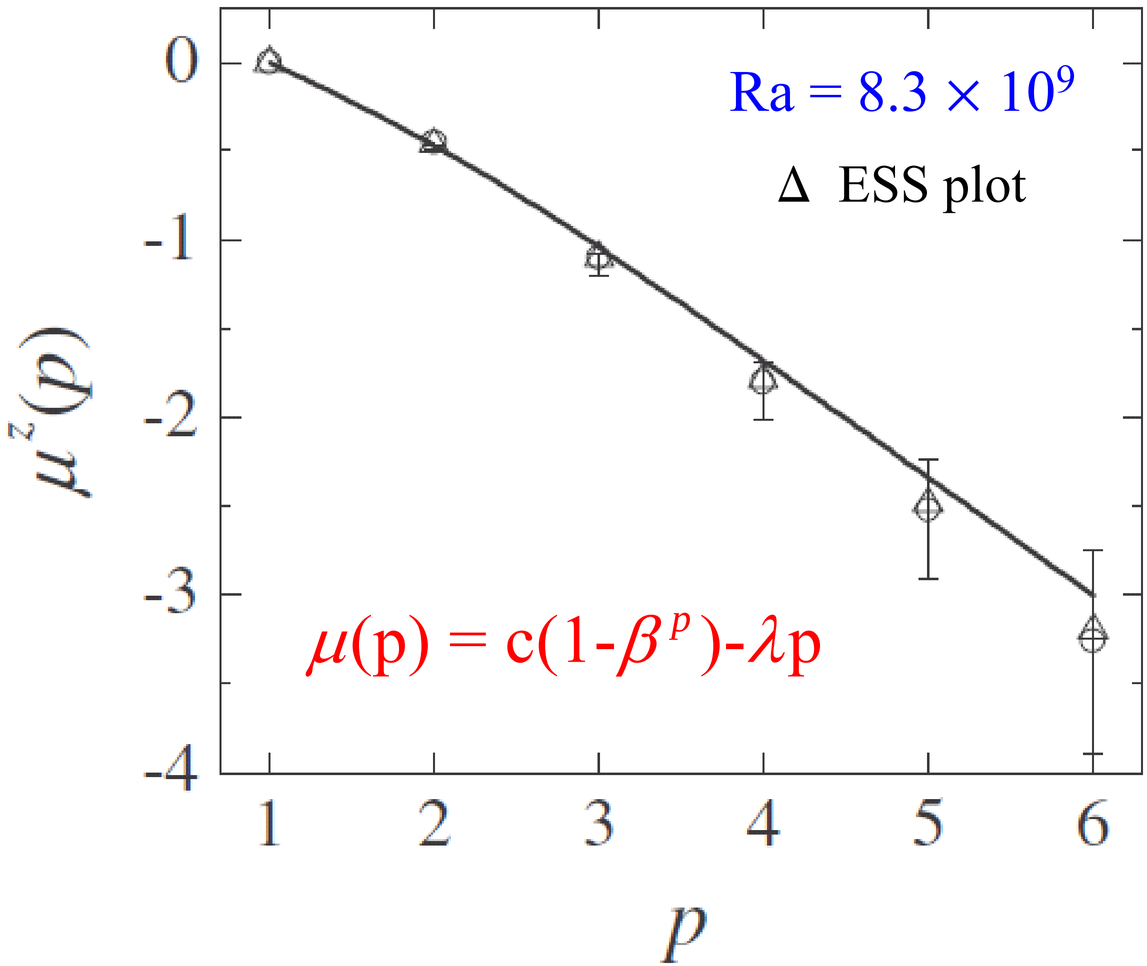

Central: c = 1 (sheet-like), $\beta = 1/3$ and $\lambda = 2/3$ (passive)

Scaling of $\langle(\varepsilon_\tau^x)^p\rangle$ and $\langle(\varepsilon_\tau^y)^p\rangle$ at the cell center:

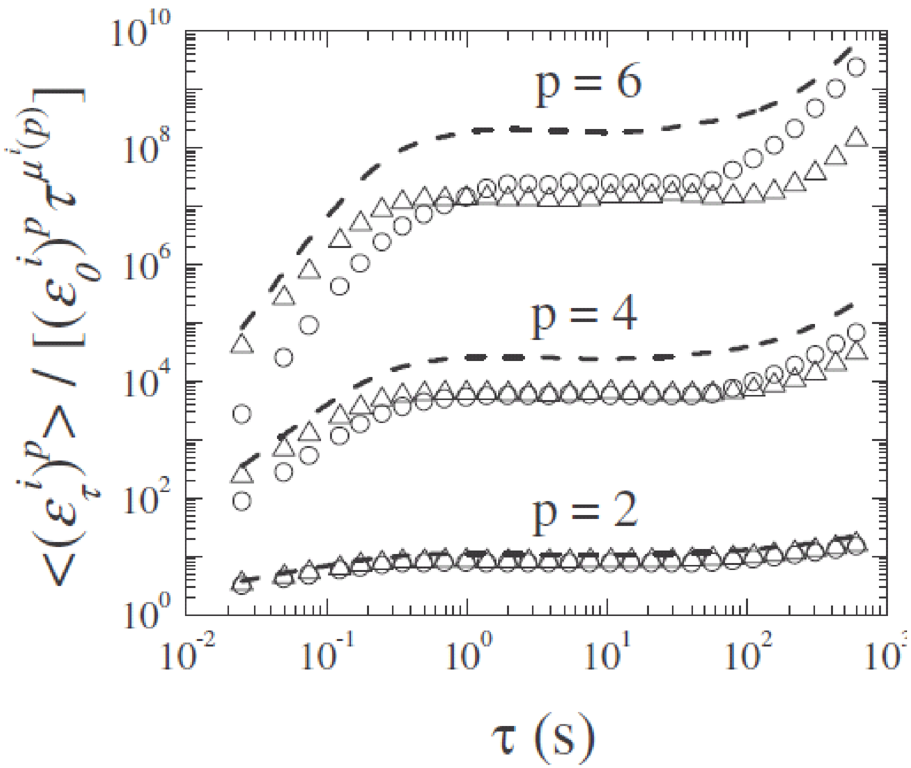

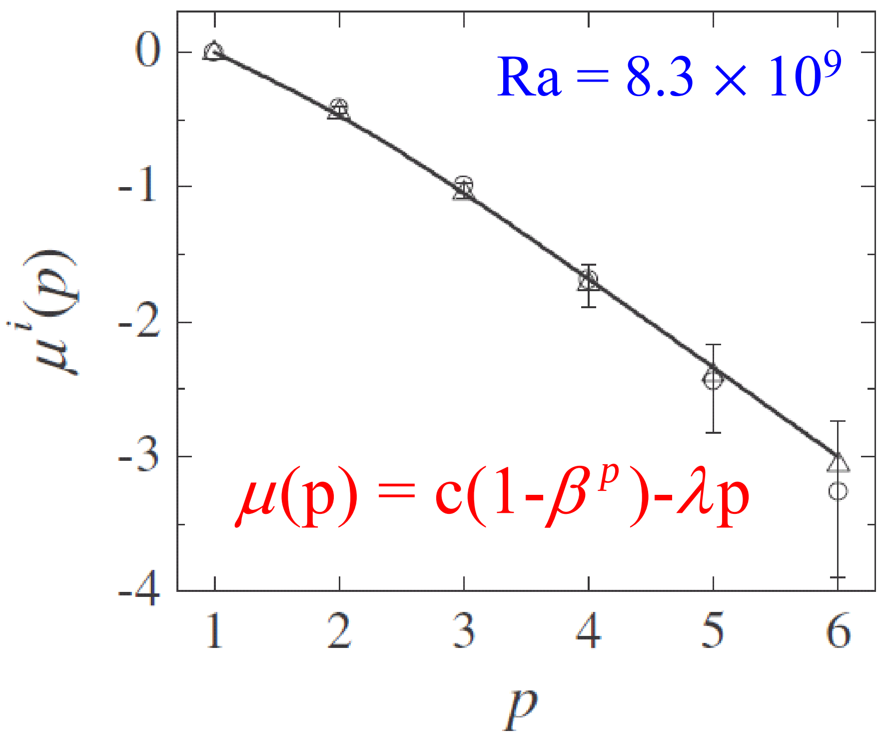

In the central region, μ^x(p) and μ^y(p) are the same as μ^z(p):

c = 1 (sheet-like), β = 1/3 and λ = 2/3 (passive)

Scaling of $\langle(\varepsilon_\tau^i)^p\rangle$ near the sidewall:

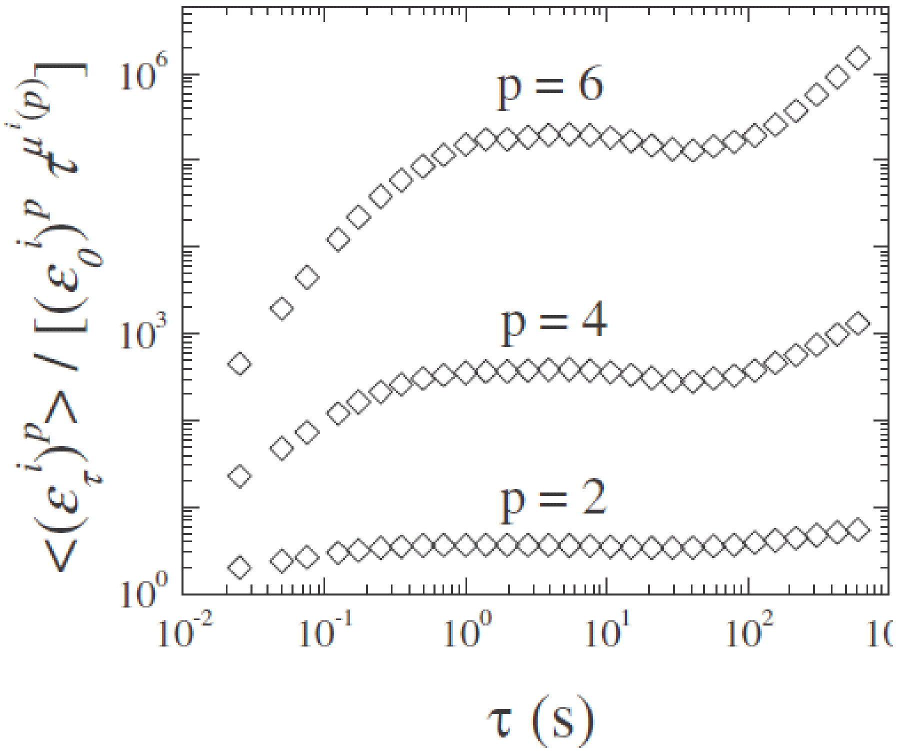

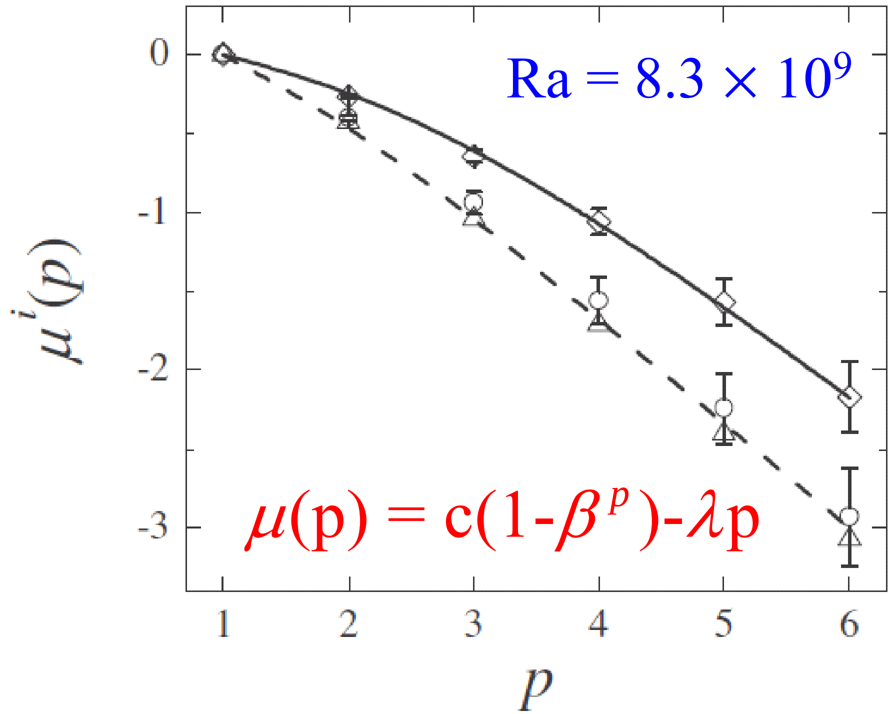

x and y components: c = 1 (sheet-like), β = 1/3 and λ = 2/3 (passive)

z-component: c = 2 (filament-like), β = 2/3 and λ = 2/3 (passive)

Temperature profile and histogram of the temperature gradient components near the thermal boundary layer

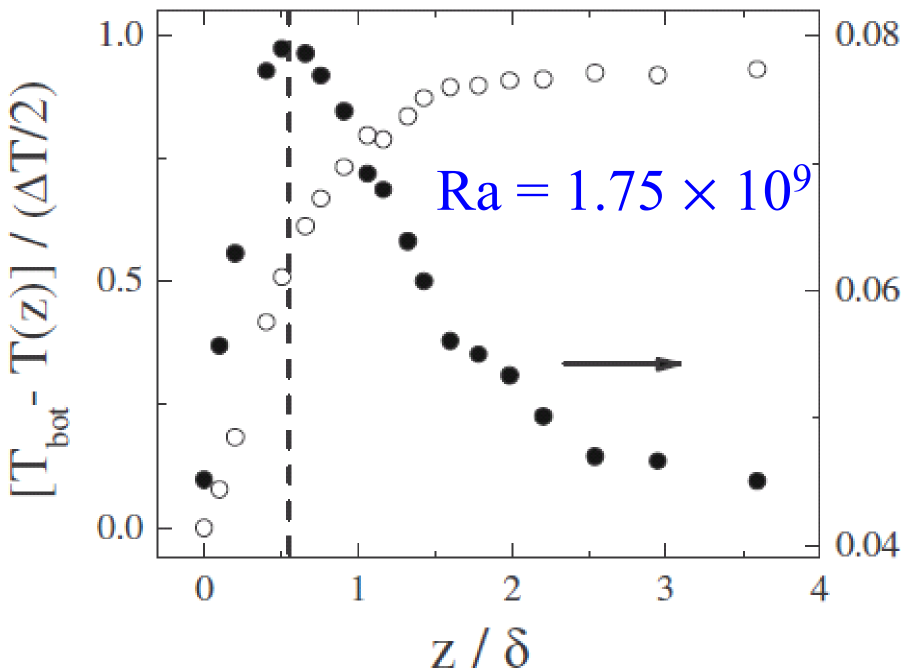

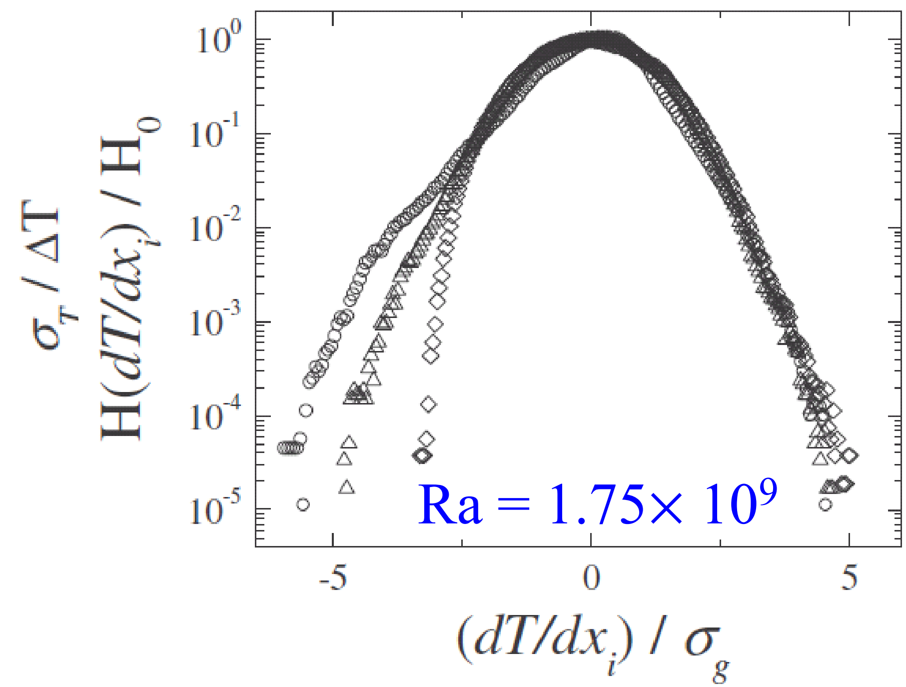

Temperature fluctuations near the lower conducting plate are governed by the thermal boundary layer thickness, δ, which decreases with increasing Ra. Measurements were made in the peak region ($0.5 \leq z/\delta \leq 0.9$).

Scaling of $\langle(\varepsilon_\tau^i)^p\rangle$ near the lower conducting plate:

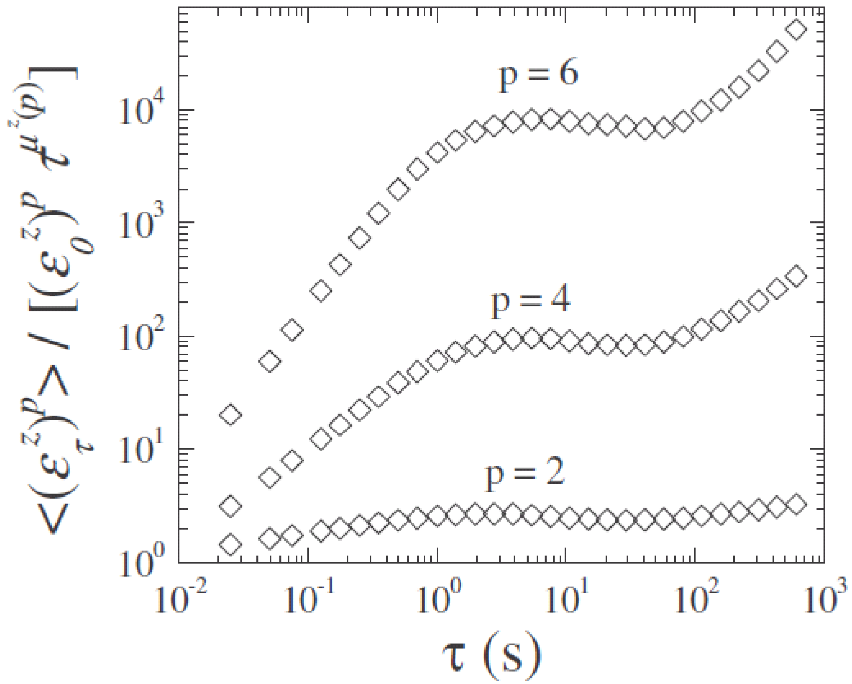

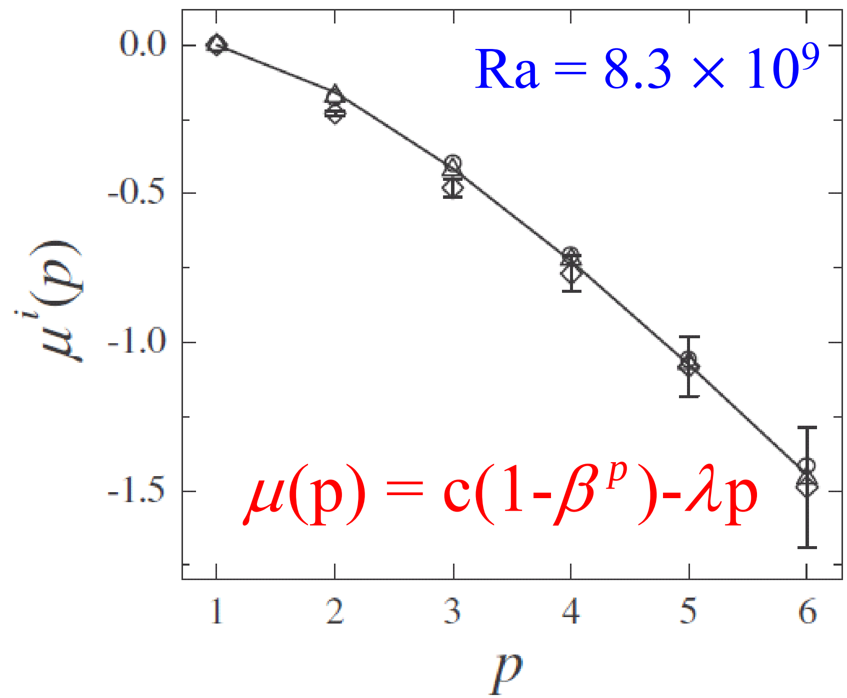

Local Bolgiano time $\tau_B \approx \tau_0 \, L_B(0)/L \approx 3.5$ s.

Inside the thermal boundary layer (all components):

c = 1 (sheet-like), $\beta = 3/5$ and $\lambda = 2/5$ (active)

Scaling exponent μ(p) of the total dissipation:

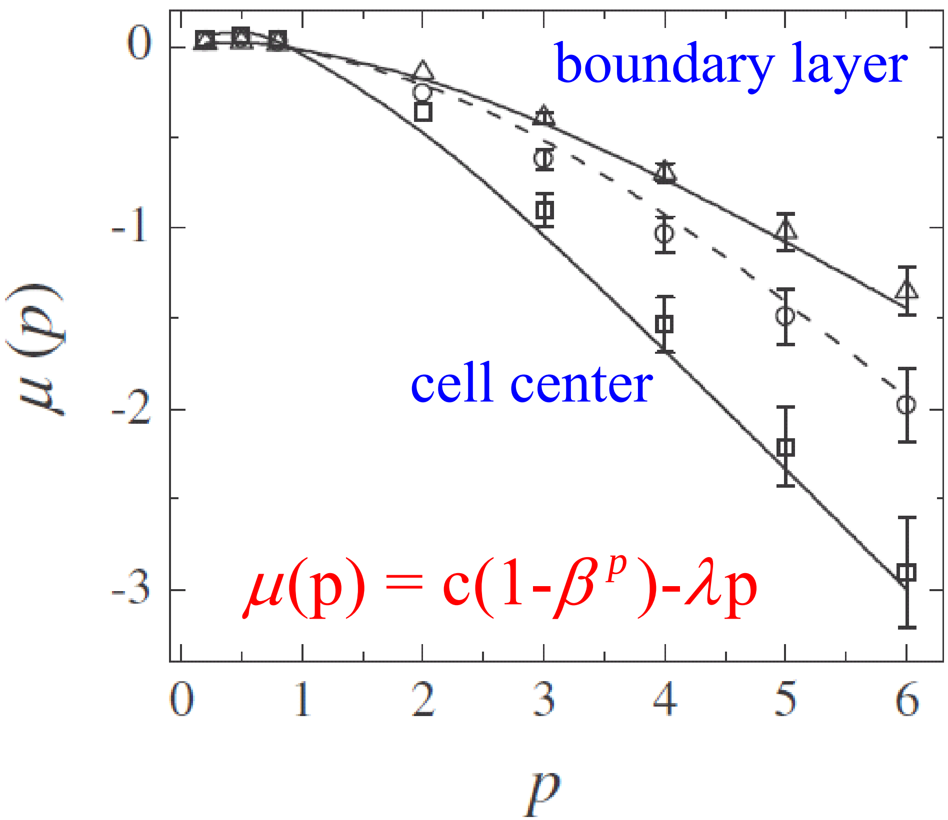

Ra = 8.3×10^9

Sidewall: c = 2.4 (sheet-like), $\beta = 0.72$ and $\lambda = 2/3$ (passive)

Evolution of μ(p) along the central axis

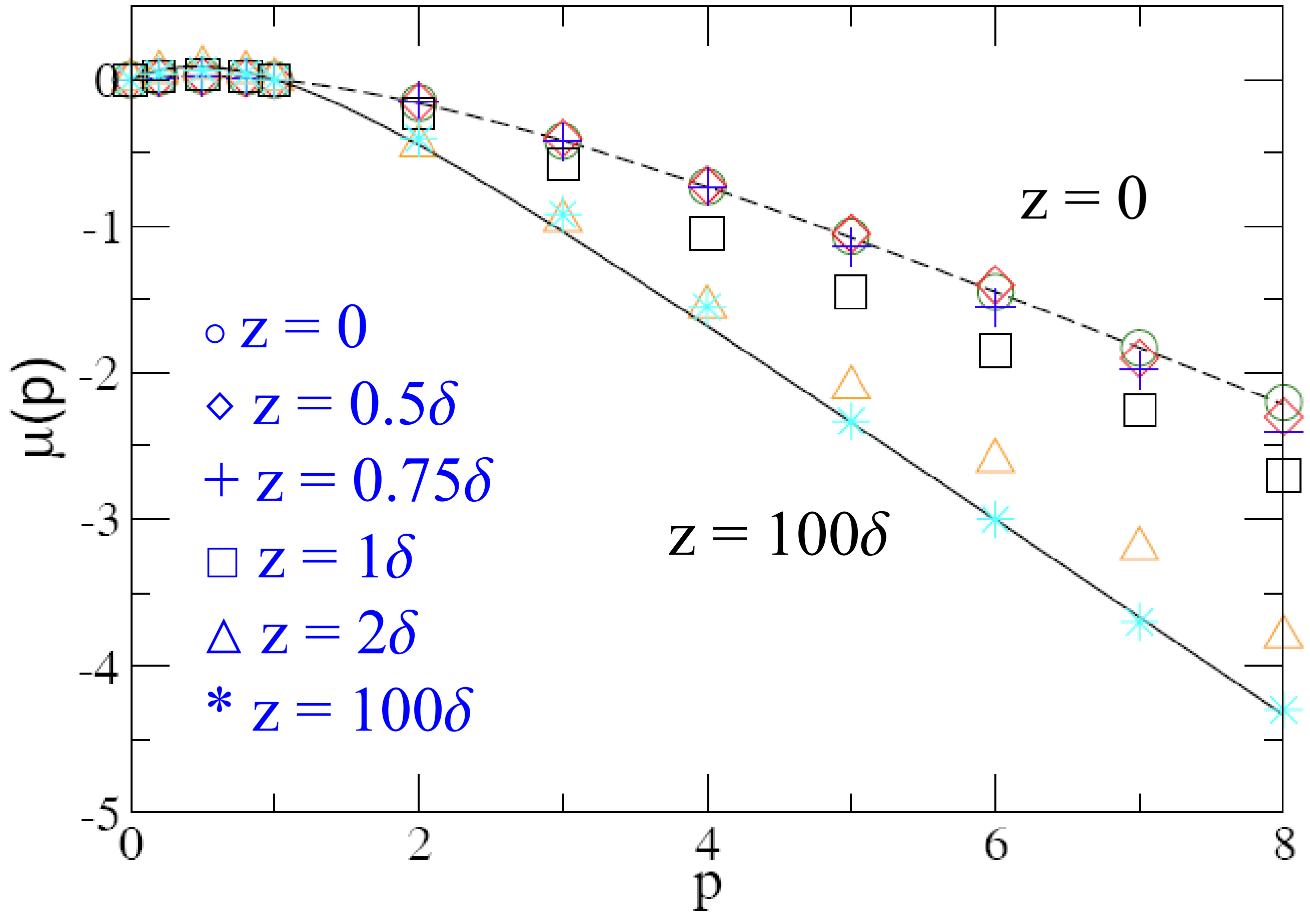

$$\mu(p) \;=\; c(1-\beta^{p})-\lambda p = 1-[1-\lambda(z)]^{p}-\lambda(z)\,p$$

D. Relation between temporal and spatial fluctuations

$$\varepsilon_\tau^i(\mathbf{r},\mathrm{t}) = \frac{1}{\tau}\int_t^{t+\tau} \kappa[\partial_i T_f(\mathbf{r},\mathrm{t'})]^2 \mathrm{dt}' \Leftrightarrow \varepsilon_r^i(\mathbf{x},\mathrm{t}) = \frac{1}{\frac{4\pi}{3} r^3}\int_0^r \kappa[\partial_i T_f(\mathbf{r}',\mathrm{t})]^2 \mathrm{dr}'$$

Equal-time velocity correlation function:

$$C_u(r,0) = \frac{\langle u(x,t)\ u(x+r,t)\rangle_t}{(\sigma_u)_1 (\sigma_u)_2}$$

or energy spectrum

$$E_u(k) = \int_{-\infty}^{\infty} C_u(r,0)\, e^{-ikr} dr$$

Velocity structure functions:

$$S_u^{(p)}(r) = \left\langle ([\mathbf{u}(x+r,t) - \mathbf{u}(x,t)]\bullet\frac{\mathbf{r}}{r})^p \right\rangle_t$$

Single-point time series measurements (LDV, hot wire, …):

(i) Temporal velocity correlation function:

$$C_u(0,\tau) = \frac{\langle u(x,t)\,u(x,t+\tau)\rangle_t}{(\sigma_u)_1(\sigma_u)_2}$$

or frequency power spectrum:

$$E_u(f) = \int_{-\infty}^{\infty} C_u(0,\tau)\, e^{-i2\pi f\tau} d\tau$$

(ii) Temporal velocity structure functions:

$$S_u^{(p)}(\tau) = \langle [u(x,t+\tau) - u(x,t)]^p \rangle_t$$

Two-point time series measurements (PIV or two local probes):

Velocity space-time cross-correlation function:

$$C_u(r,\tau) = \frac{\langle u(x,t)u(x+r,t+\tau)\rangle_t}{(\sigma_u)_1(\sigma_u)_2}$$

Taylor's frozen flow hypothesis:

$$u(x,t) \rightleftharpoons u(x+U_0\tau, t+\tau)$$

Then we have

$$C_u(r,\tau) = \frac{\langle u(x+U_0\tau, t+\tau)\ u(x+r,t+\tau)\rangle_t}{(\sigma_u)_1(\sigma_u)_2} = C_u(r_T, 0)$$

with $\quad r_T = r - U_0\tau$

Requirement for Taylor's hypothesis: $U_0 >> (\sigma_u)_i$

Elliptic model of He and Zhang (Phys. Rev. E, 2006)

$$C_u(r,\tau)=C_u(0,0)+\cancel{\frac{\partial C_u(0,0)}{\partial r}}r+\cancel{\frac{\partial C_u(0,0)}{\partial \tau}}\tau+\frac{\partial^2 C_u(0,0)}{\partial r\partial \tau}r\tau+\frac{1}{2}\left[\frac{\partial^2 C_u(0,0)}{\partial r^2}r^2+\frac{\partial^2 C_u(0,0)}{\partial \tau^2}\tau^2\right]$$

$$=C_u(0,0)+\frac{1}{2}\frac{\partial^2 C_u(0,0)}{\partial r^2}r_E^2=C_u(0,0)-\left(\frac{r_E}{\lambda_u}\right)^2=C_u(r_E,0)$$

$$r_E^2=(r-U\tau)^2+V^2\tau^2$$

$$U=-\frac{\partial^2 C_u(0,0)}{\partial r\partial \tau}\left[\frac{\partial^2 C_u(0,0)}{\partial r^2}\right]^{-1}=U_0$$

$$V^2=\frac{\partial^2 C_u(0,0)}{\partial \tau^2}\left[\frac{\partial^2 C_u(0,0)}{\partial r^2}\right]^{-1}-U^2=(s\lambda_u)^2+\sigma_u^2$$

$$\lambda_u=\left[-\frac{1}{2}\frac{\partial^2 C_u(0,0)}{\partial r^2}\right]^{-1/2}$$

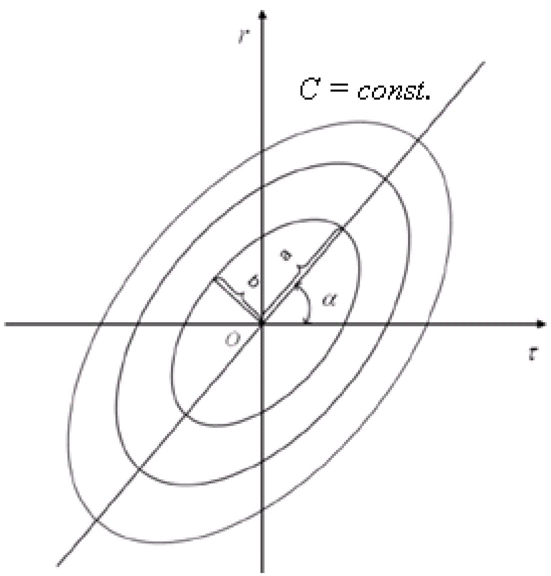

iso-correlation contours

Two-point temperature measurements over varying distance r

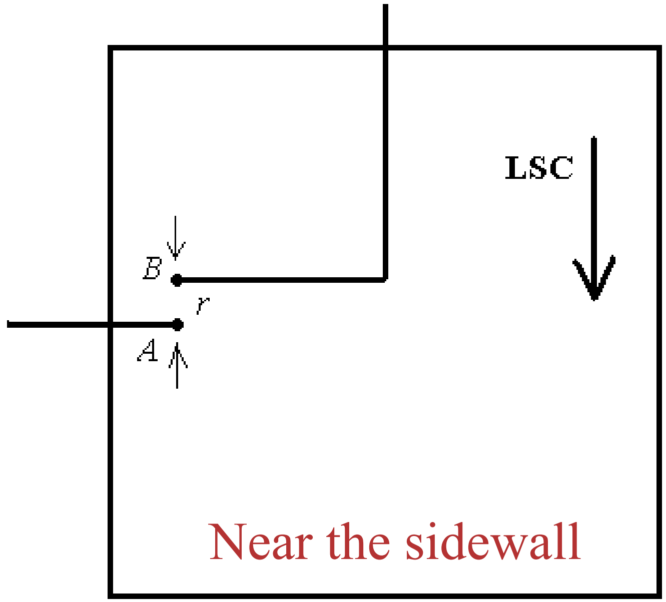

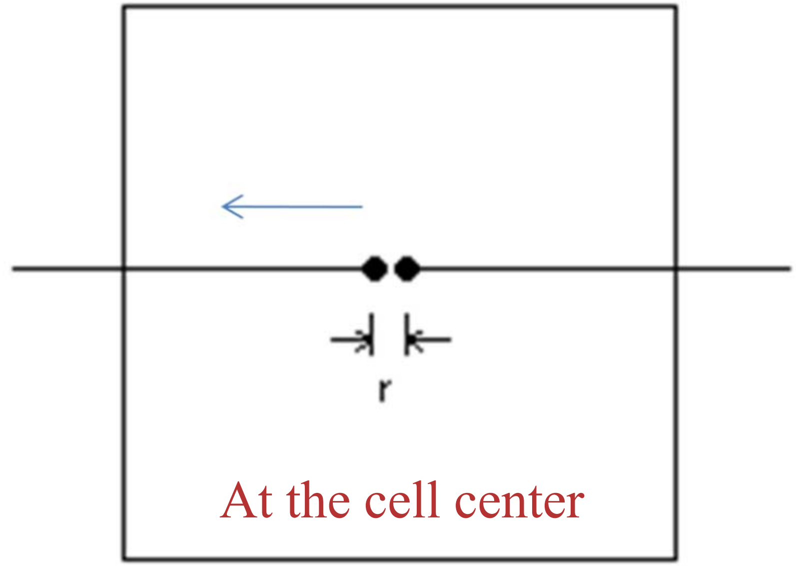

Temperature space-time cross-correlation function:

$$C_T(r,\tau) = \frac{\langle T(x,t)\ T(x+r,t+\tau)\rangle_t}{(\sigma_T)_1 (\sigma_T)_2}$$

Temperature is a passive scalar in the bulk region, and thus $C_T(r,\tau)$ is expected to have the same scaling form as $C_u(r,\tau)$ does.

Experimental results near the sidewall

3-D plot of the measured $C_T(r,\tau)$

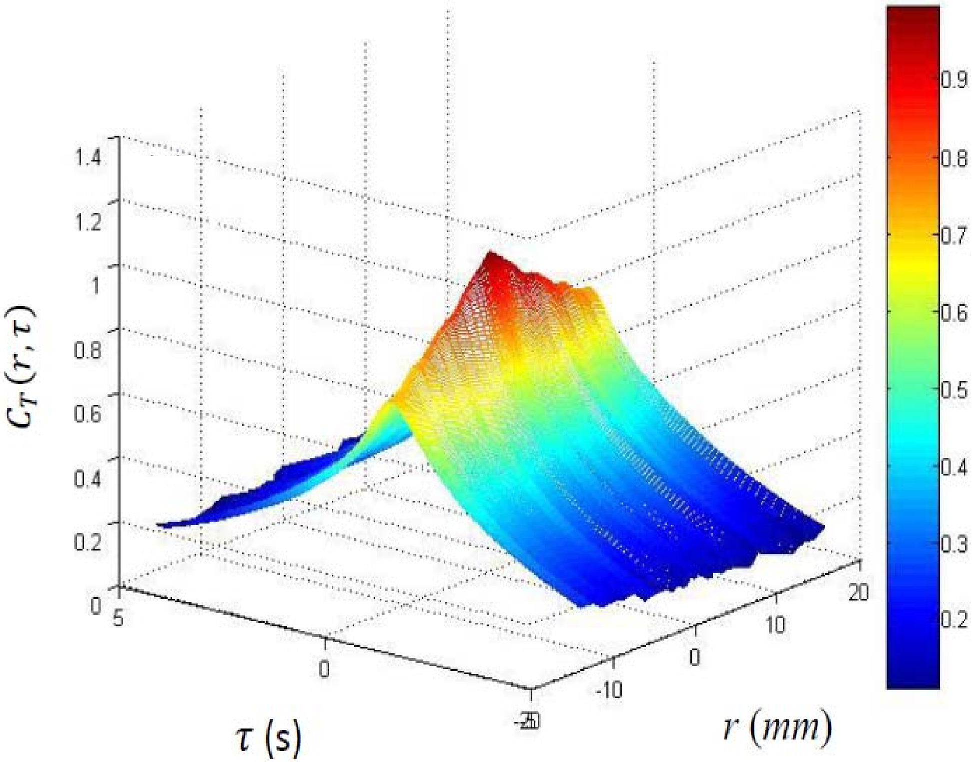

2-D plot of iso-correlation contours

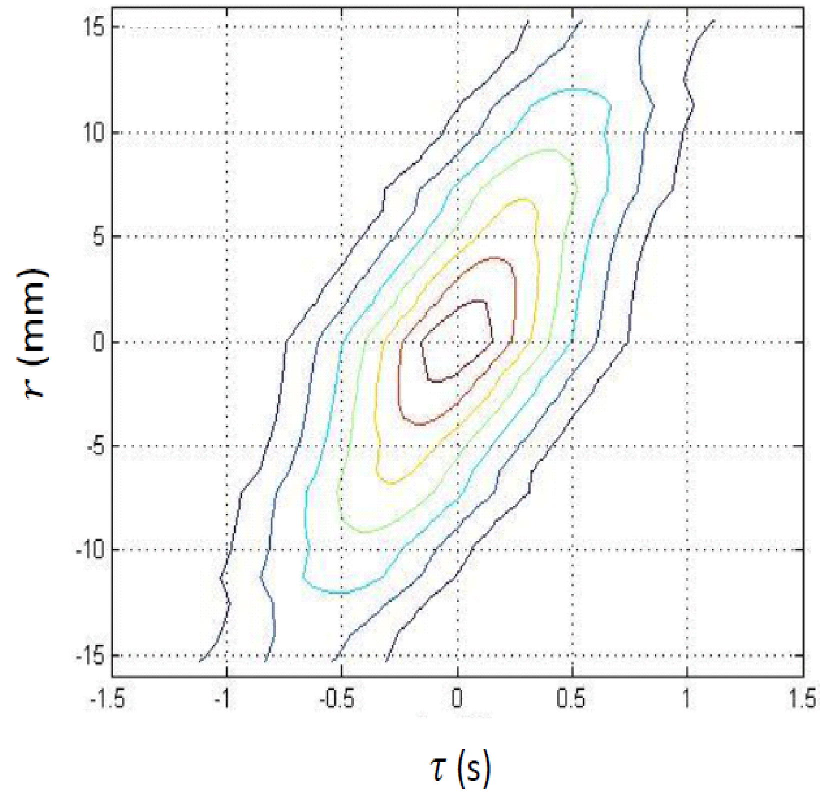

Experiment confirms the elliptic model:

$$C_T(r,\tau) = C_T(r_E, 0)$$

$$r_E^2 = (r - U\tau)^2 + V^2\tau^2$$

He, He and Tong, Phys. Rev. E, **81**, 065303(R), 2010.

Elliptic model

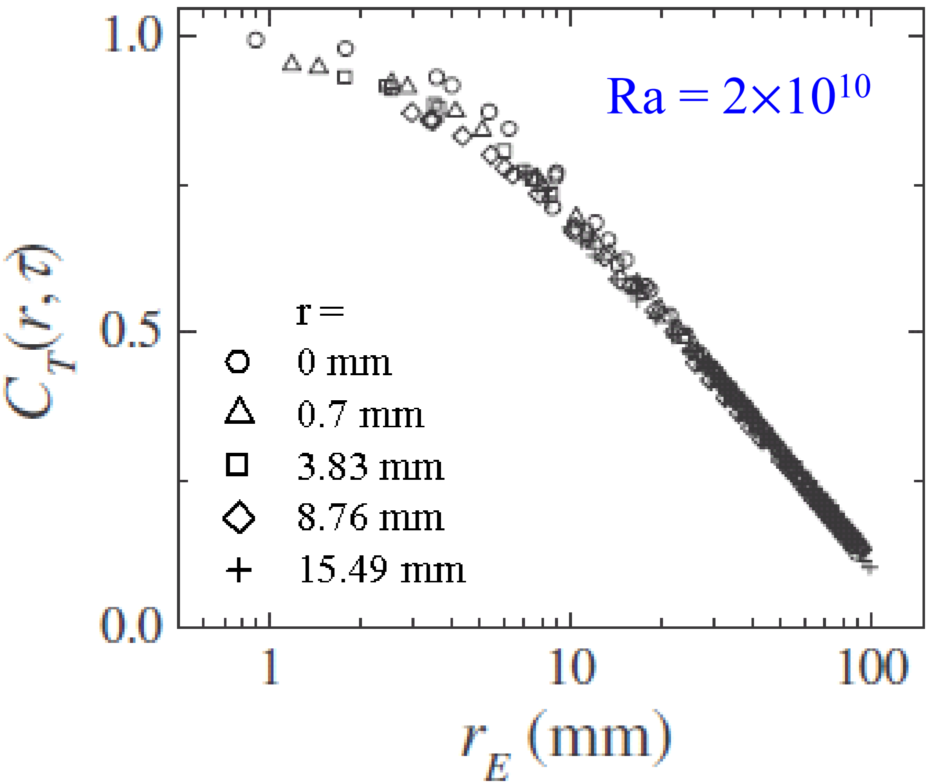

$$r_E^2 = (r - U\tau)^2 + V^2\tau^2$$

$$C(r,\tau) = C(r_E, 0)$$

Taylor's hypothesis

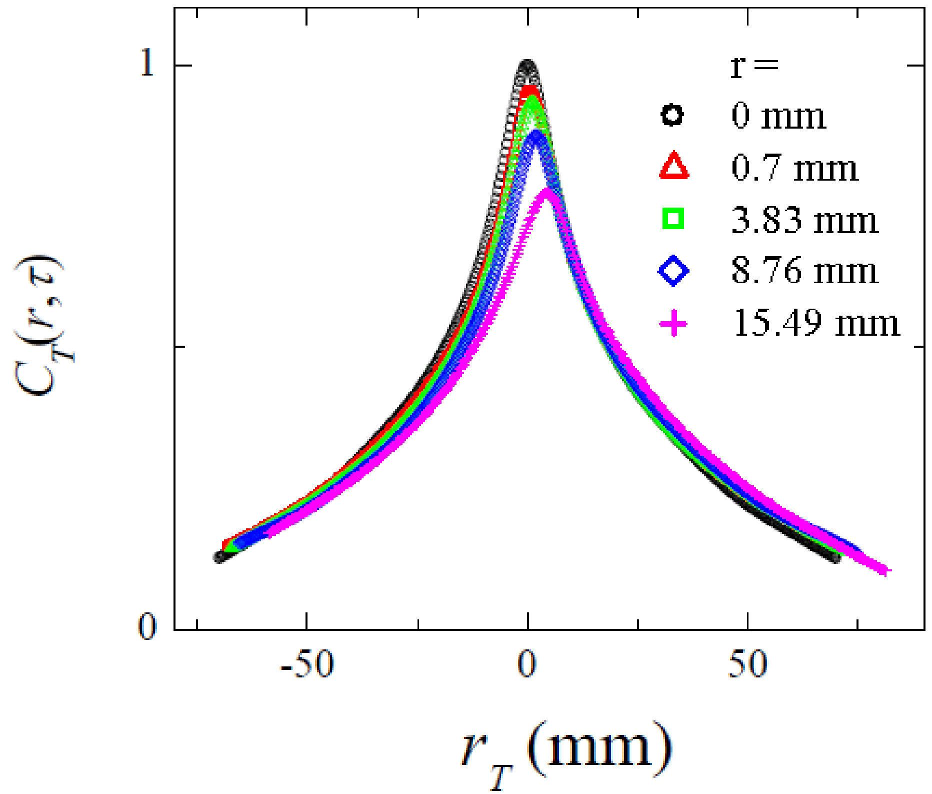

$$r_T = r - U\tau$$

$$C(r,\tau) = C(r_T, 0)$$

Taylor's hypothesis does not hold

Single-point temperature measurement ($r = 0$): $C_T(0,\tau) = C_T(r_E, 0)$

$r_E = \sqrt{U^2 + V^2}\,\tau$ Power spectrum: $E_T(f) = \int_{-\infty}^{\infty} C_T(0,\tau) e^{-2\pi i f \tau} d\tau$

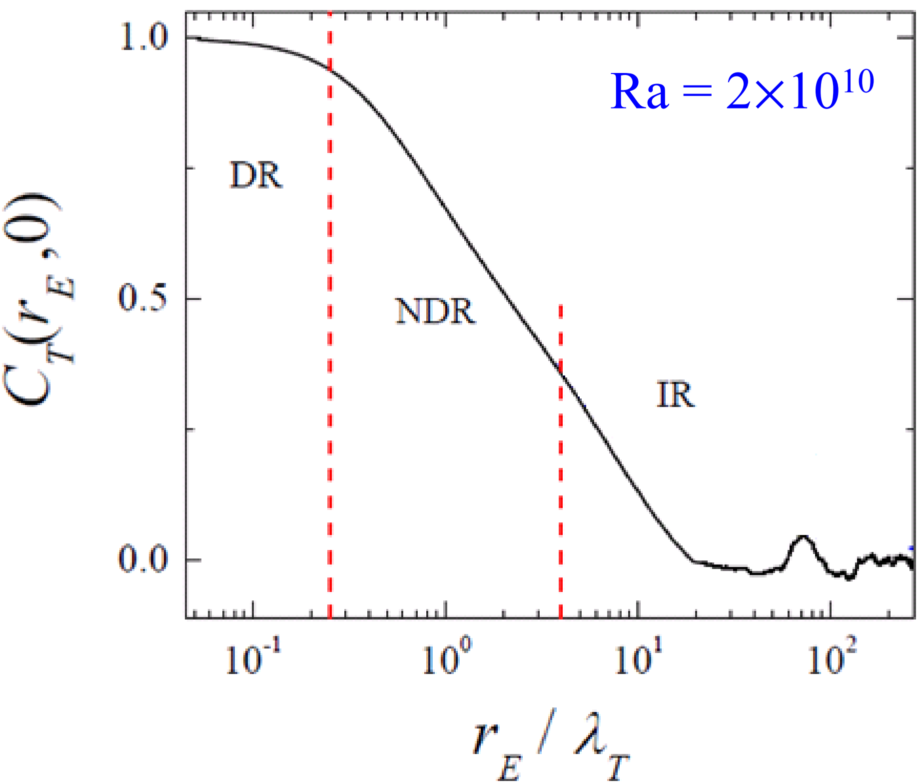

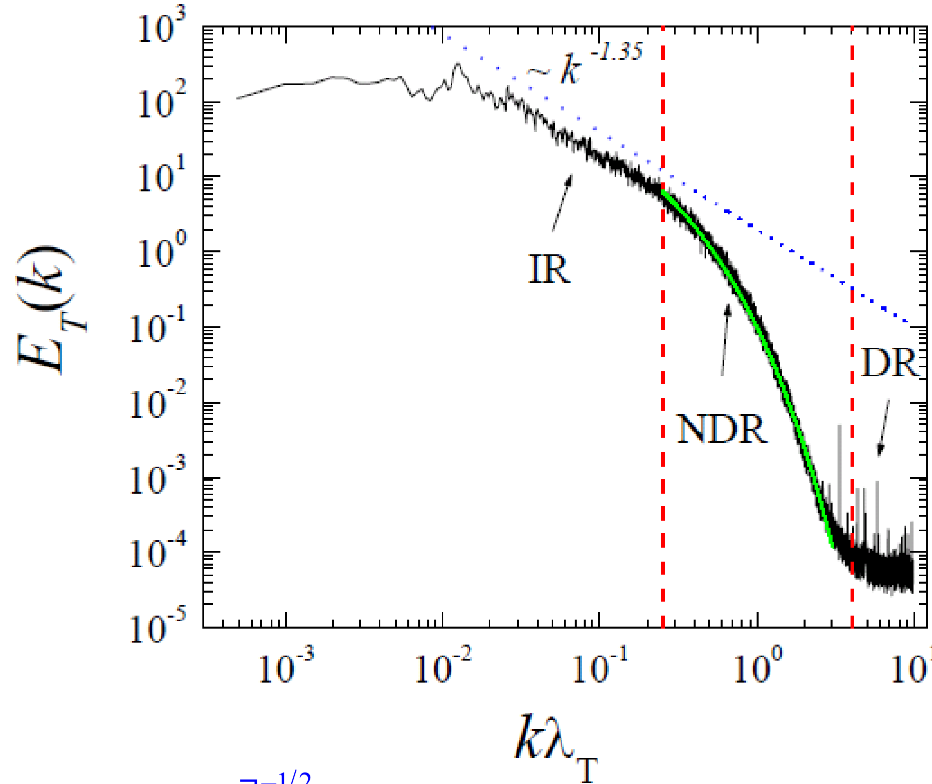

Taylor's micro-scale: $\lambda_T = \left[-\frac{1}{2} \frac{\partial^2 C_T(0,0)}{\partial r^2} \right]^{-1/2} = 8.53 \text{ mm}$

Reynolds number: $\mathrm{Re}_{\lambda_T} \approx \left(U^2 + V^2\right)^{1/2} \lambda_T / \nu \approx 240$

Experimental results at the cell center

3-D plot of the measured $C_T(r,\tau)$

2-D plot of iso-correlation contours

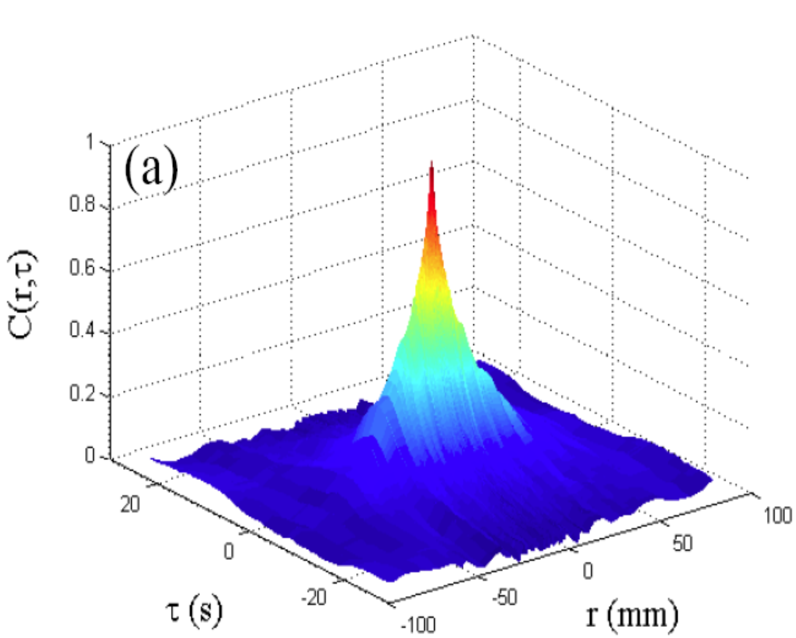

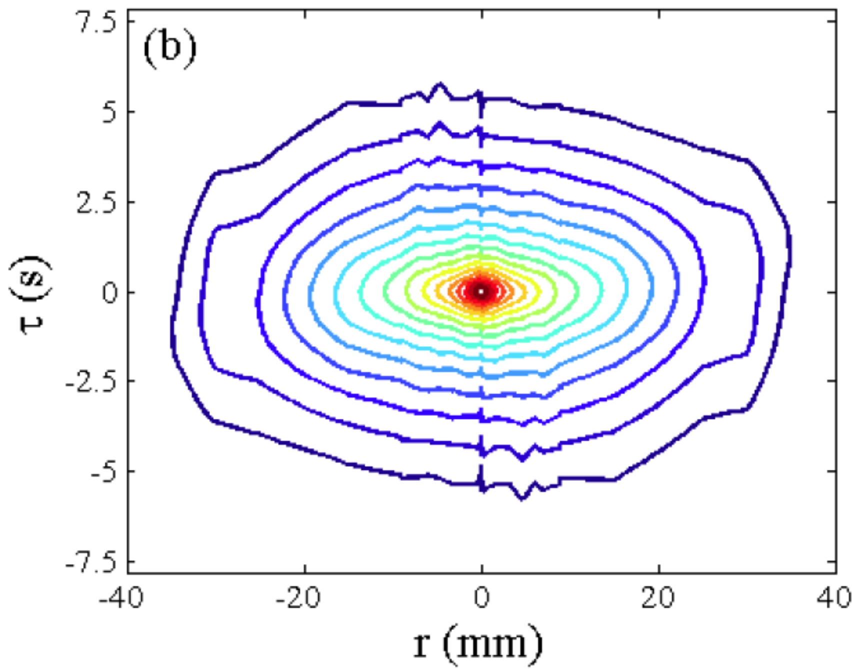

Experiment confirms the elliptic model:

$$C_T(r,\tau) = C_T(r_K, 0) \quad \text{with} \quad r_K^2 = r^2 + V^2\tau^2 \quad \text{or} \quad \frac{r^2}{a^2} + \frac{\tau^2}{b^2} = 1$$

He and Tong, Phys. Rev. E, **83**, 037302 (2011).

Scaling behavior of $C_T(r,\tau)$ in the central region of the cell

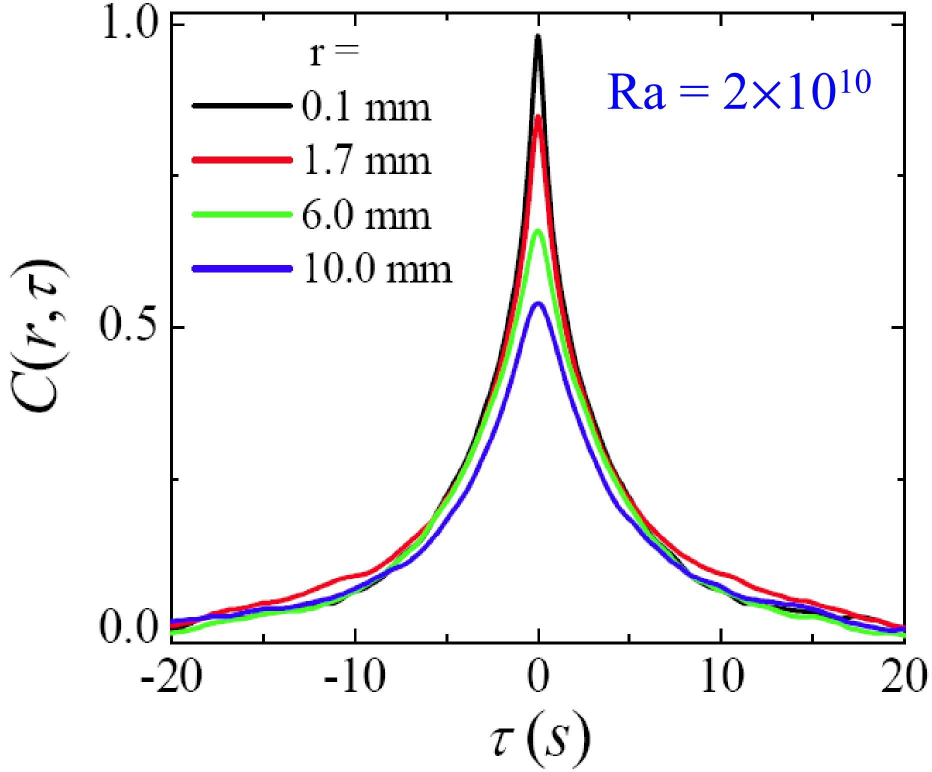

Measured mean velocity:

$U_0 = 0$

and rms velocity:

$\sigma_u = 8$ mm/s

Symmetric shape with $\tau_p = \dfrac{U}{U^2 + V^2} r \;\rightarrow\; U = 0$ and $V = 8.5$ mm/s

Kraichnan's random sweeping hypothesis is valid in the inner region.

Comparison between $C_T(r_E,0)$ and $C_T(r,0)$ in the bulk region

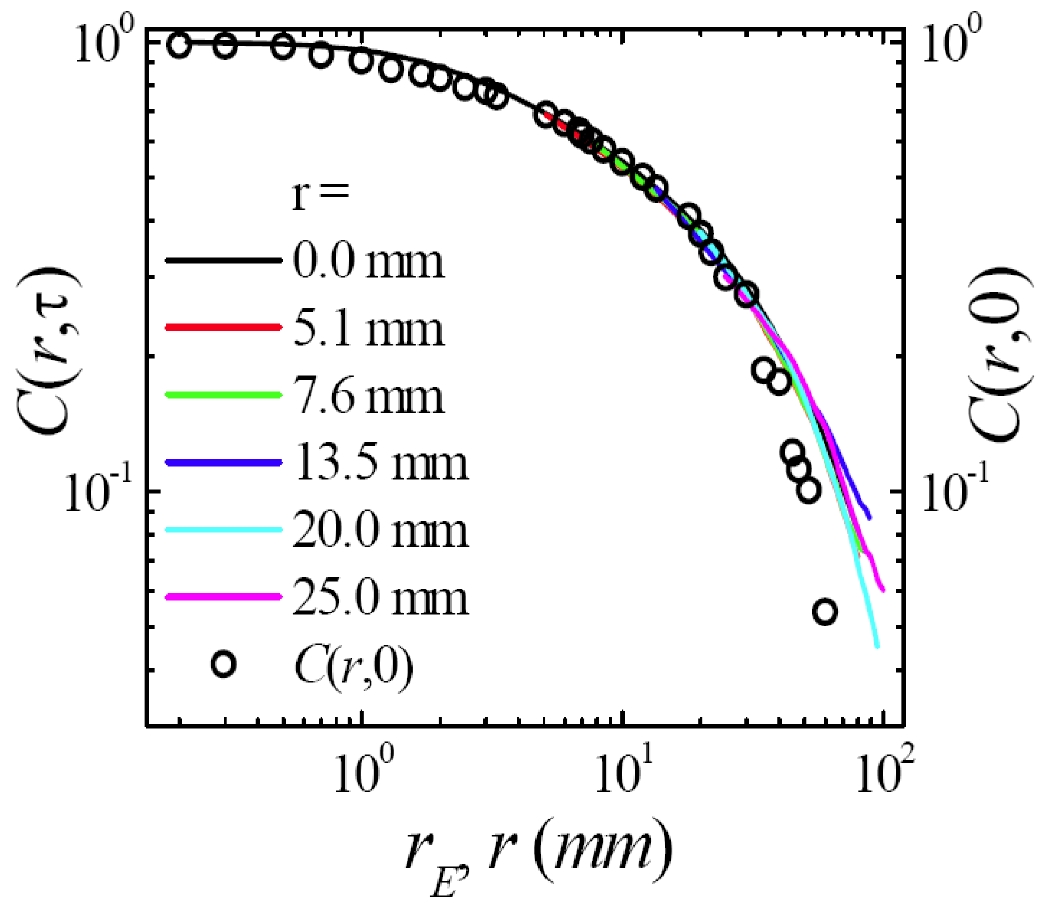

Ra = 2×10^10

$$r_E^2 = \left(r - U(r)\tau\right)^2 + V^2(r)\tau^2$$

Connection of time-domain results to the theory in spatial domain

Show that

$$\varepsilon_\tau^i(\mathbf{r},\mathrm{t}) = \frac{1}{\tau}\int_t^{t+\tau} \kappa[\partial_i T_f(\mathbf{r},\mathrm{t}')]^2 \mathrm{dt}' \cong \varepsilon_r^i(\mathbf{x},\mathrm{t}) = \frac{1}{\frac{4\pi}{3}r^3}\int_0^r \kappa[\partial_i T_f(\mathbf{r}',\mathrm{t})]^2 \mathrm{dr}'$$

Given that $C_T(r,\tau) = C_T(r_E,0)$ with $r_E^2 = (r - U\tau)^2 + V^2\tau^2$

- At the cell center, we have $r_E = V\tau$ (r = 0) and the average over $d\tau$ (or dt) is equivalent to the average over dr_E (average over a sphere of radius $r_E = Vt$).

- Near the sidewall, we have $r_E = (U^2+V^2)^{1/2}\,\tau$ (r = 0) and the average over $d\tau$ (or dt) is equivalent to the average over dr_E (average over a ellipsoid of major axis $r_E = (U^2+V^2)^{1/2}\,\tau$ and minor axis $r_E = Vt$).

4. Summary

- Measured thermal dissipation field has the form $\epsilon_T(\mathbf{r}) = \epsilon_m(\mathbf{r}) + \epsilon_f(\mathbf{r})$, with $\epsilon_m(\mathbf{r})$ concentrating in the thermal boundary layers and $\epsilon_f(\mathbf{r})$ occupying mainly in the plume-dominated bulk region.

- Measured $\epsilon_f(\mathbf{r}) \sim \mathrm{Ra}^{-0.33}$ in the bulk region and $\epsilon_m(\mathbf{r}) \sim \mathrm{Ra}^{+0.63}$ inside the thermal boundary layer.

- Measured moments have the power-law form $\langle(\varepsilon_\tau^i)^p\rangle \sim \tau^{\mu^i(p)}$ with $\mu^i(\mathrm{p}) = \mathrm{c}(1\text{-}\beta^p)\text{-}\lambda\mathrm{p}$ for all three temperature gradient components and for all values of p up to 6 and are observed at three representative locations in the cell.

- Scaling of $\langle(\varepsilon_\tau^i)^p\rangle$ contains two contributions: (i) the horizontal exponents $\mu^i(p)$ ($i = x,y$) have the same parameters in the bulk region: $c = 1$ (sheet-like) and $\lambda = 2/3$ (passive scalar) but become $c = 1$ (sheet-like) and $\lambda = 2/5$ (active scalar) in the thermal boundary layer.

- (ii) Superimposed on this background is the vertical exponent $\mu^z(p)$, which varies with the position. At the cell center and inside the thermal boundary layer, $\mu^z(p)$ remains the same as the two horizontal exponents, whereas near the sidewall, $\mu^z(p)$ becomes different from $\mu^i(p)$ ($i = x,y$) with the parameters $c = 2$ (filament-like) and $\lambda = 2/3$ (passive scalar).

- Measured temperature space-time cross-correlation function $C_T(r, \tau)$ near the sidewall and at the cell center both has the scaling form $C_T(r_E,0)$, as predicted by the elliptic model.

- The new scaling relation, $r_E^2 = (r\text{-}U\tau)^2 + V^2\tau^2$, can be applied to a large class of turbulent flows, such as turbulent wind tunnels, in which there are two characteristic velocities associated with the mean and rms velocities.